

Cross sections for 2-to-3 meson-meson scattering

Wan-Xia Li¹, Xiao-Ming Xu¹, and H. J. Weber²

¹Department of Physics, Shanghai University, Baoshan, Shanghai 200444, China

²Department of Physics, University of Virginia, Charlottesville, VA 22904, USA

Abstract

We study 2-to-3 meson-meson scattering based on the process that a gluon is created from a constituent quark or antiquark and subsequently the gluon creates a quark-antiquark pair. The transition potential for the process is derived in QCD. Eight Feynman diagrams at tree level are involved in the 2-to-3 meson-meson scattering. Starting from the S -matrix element, we derive the unpolarized cross section from the eight transition amplitudes corresponding to the eight Feynman diagrams. The transition amplitudes contain color, spin, and flavor matrix elements. The 2-to-3 meson-meson scattering includes $\pi\pi \rightarrow \pi K \bar{K}$, $\pi K \rightarrow \pi\pi K$, $\pi K \rightarrow K K \bar{K}$, $K K \rightarrow \pi K K$, and $K \bar{K} \rightarrow \pi K \bar{K}$. Cross sections for the reactions are calculated. The cross sections depend on temperature obviously, and the cross section for $\pi K \rightarrow \pi\pi K$ for total isospin $I = 3/2$ at zero temperature is compared to experimental data. By comparison with inelastic 2-to-2 meson-meson scattering, we find that 2-to-3 meson-meson scattering may be as important as inelastic 2-to-2 meson-meson scattering.

Keywords: Inelastic meson-meson scattering, Quark-antiquark creation, Relativistic constituent quark potential model.

PACS: 13.75.Lb; 12.39.Jh; 12.39.Pn

I. INTRODUCTION

Many experiments and analyses have been done for elastic $\pi\pi$ scattering, elastic πK scattering, and elastic $K \bar{K}$ scattering. Elastic phase shifts and elastic cross sections for

$\pi\pi$ scattering have been measured via $\pi^- p \rightarrow \pi^- \pi^- \Delta^{++}$ [1–3], $\pi^+ p \rightarrow \pi^0 \pi^0 \Delta^{++}$ [4], $\pi^+ p \rightarrow \pi^+ \pi^+ n$ [5–7], $\pi^- p \rightarrow \pi^0 \pi^0 n$ [8], $\pi^- d \rightarrow \pi^- \pi^- pp$ [9, 10], $\pi^+ p \rightarrow \pi^+ \pi^- \Delta^{++}$ [11], $\pi^\pm p \rightarrow \pi^\pm \pi^0 p$ [7, 12, 13], $\pi^- p \rightarrow \pi^- \pi^+ n$ [7, 14–21], and $K^\pm \rightarrow \pi^+ \pi^- e^\pm \nu$ [22–25]. When the total isospin of the two pions is 0 or 1, from phase shifts and cross sections one can identify resonances such as $f_0(980)$, $f_2(1270)$, $f_0(1370)$, $a_0(980)$, and $\rho(1450)$. When the total isospin equals 2, the cross section for elastic $\pi\pi$ scattering can go up to 12 mb. Elastic phase shifts and elastic cross sections for πK scattering have been measured via $K^\pm p \rightarrow K^\pm \pi^- \Delta^{++}$ [26–29], $K^+ p \rightarrow K^0 \pi^0 \Delta^{++}$ [26], $K^\pm p \rightarrow K^\pm \pi^+ n$ [29, 30], and $D^+ \rightarrow K^- \pi^+ e^+ \nu_e$ [31]. From elastic πK scattering with a total isospin of 1/2, one can find resonances such as $K_0^*(1430)$. The cross section for elastic πK scattering with the other total isospin 3/2 may become as large as 4.6 mb. The elastic cross section for $K^+ K^-$ scattering obtained from $\pi^+ p \rightarrow K^+ K^- \Delta^{++}$ in Ref. [11] decreases from 3.8 mb at 1 GeV to 2.9 mb at 1.38 GeV. Elastic phase shifts for $K^+ K^-$ scattering were extracted from $\pi^- p \rightarrow K^+ K^- n$ and $\pi^+ n \rightarrow K^+ K^- p$ in Ref. [32]. A variety of theoretical approaches [33–46] apply to elastic meson-meson scattering.

Experimental data on $\pi\pi \rightarrow \rho$ are given in Ref. [47] and the cross section for $\pi K \rightarrow K^*$ in vacuum was estimated in Ref. [48]. On the basis of the process that a quark in one initial meson and an antiquark in the other initial meson annihilate into a gluon and subsequently the gluon is absorbed by the other antiquark or quark, 2-to-1 meson-meson scattering has been studied in Ref. [49], and the resulting cross sections for $\pi\pi \rightarrow \rho$ and $\pi K \rightarrow K^*$ agree with the empirical data given in Refs. [47, 48]. Cross sections for the reactions $\pi^- \pi^- \rightarrow \pi^- \pi^- \pi^+ \pi^-$ and $\pi^- \pi^- \rightarrow \pi^- \pi^- \pi^0 \pi^0$ were measured in Refs. [3, 9], and the cross section goes up when the dipion mass increases from 0.8 GeV. The cross section for $\pi^- K^- \rightarrow \pi^- \pi^- K^0 + \pi^0 \pi^- K^-$ was investigated in Ref. [27]. In the present work we study 2-to-3 meson-meson scattering based on the process that a gluon is created from a quark or an antiquark in the two initial mesons, and the gluon then creates a quark and an antiquark. We note that 2-to-3 meson-meson scattering has not yet been studied in theory.

Inelastic 2-to-2 meson-meson scattering has been studied in Refs. [50–54]. The reac-

tions $\pi\pi \rightarrow K\bar{K}$, $\rho\rho \rightarrow K\bar{K}$, $\pi\rho \rightarrow K\bar{K}^*$, and $\pi\rho \rightarrow K^*\bar{K}$ can be described by effective meson Lagrangians. The cross sections for the four reactions have been obtained from the exchange of either a kaon or a vector kaon between the two colliding mesons [50, 51]. A study of $\pi\pi \rightarrow K\bar{K}$ scattering by means of partial-wave dispersion relations of the Roy-Steiner type is performed in Ref. [54], and precise parametrizations of the S , P , and D partial waves in the $\pi\pi \rightarrow K\bar{K}$ scattering amplitude are obtained from the data. To generate all the resonances with isospin 0 and masses below 2 GeV, S -wave meson-meson scattering for total isospin $I = 0$ and $1/2$ is studied in Ref. [55] with 13 coupled channels. Their S -wave phase shifts and modulus for $\pi\pi \rightarrow K\bar{K}$ for $I = 0$ agree with experimental data, and $\pi\pi \rightarrow \rho\rho$ is determined by minimal coupling. In terms of quark degrees of freedom some reactions are mainly governed by quark interchange, quark-antiquark annihilation and creation, or both. For example, $\pi\pi \rightarrow \rho\rho$ for total isospin $I = 2$ and $\pi K \rightarrow \rho K^*$ for $I = 3/2$ involve quark interchange [52]; $\pi\pi \rightarrow \rho\rho$ for $I = 1$ and $\pi\rho \rightarrow K\bar{K}^*$ involve quark-antiquark annihilation and creation [53]; $\pi\pi \rightarrow \rho\rho$ for $I = 0$ and $\pi K \rightarrow \rho K^*$ for $I = 1/2$ involve quark interchange as well as quark-antiquark annihilation and creation [49, 53]. The reactions governed by quark interchange as well as quark-antiquark annihilation and creation have the characteristic feature that close to threshold quark interchange dominates the reactions near the critical temperature, and in the other energy region quark-antiquark annihilation and creation may dominate the reactions.

In hadronic matter created in relativistic heavy-ion collisions at the Relativistic Heavy Ion Collider and at the Large Hadron Collider, thermal equilibrium is established by elastic meson-meson scattering. Since inelastic meson-meson scattering alters the meson number, chemical equilibrium is determined by inelastic meson-meson scattering. Exactly how thermal equilibrium is established and how chemical equilibrium is established are two important issues of hadronic matter. In lead-lead collisions and in xenon-xenon collisions at the Large Hadron Collider, meson momentum measured by the ATLAS Collaboration, the CMS Collaboration, and the ALICE Collaboration goes up to 1000 GeV/ c [56–58]. A meson of such large momenta in collision with another meson in hadronic matter may yield three or more mesons. Two-to-three meson-meson scattering affects chemical equilibrium.

Therefore, we need to study the 2-to-3 meson-meson scattering in hadronic matter.

This paper is organized as follows. In Sect. II we present eight Feynman diagrams for 2-to-3 meson-meson scattering, the transition amplitudes corresponding to the eight diagrams, and cross sections related to the transition amplitudes. In Sect. III we derive a transition potential for the process that a gluon is created from a quark or an antiquark and the gluon creates a quark and an antiquark. In Sect. IV we calculate color, spin, and flavor matrix elements in the transition amplitudes. In Sect. V numerical cross sections are presented and relevant discussions are given. In Sect. VI we summarize the present work.

II. CROSS-SECTION FORMULAS

Meson A contains quark q_1 and antiquark \bar{q}_1 , and meson B has quark q_2 and antiquark \bar{q}_2 . In the collision of mesons A and B a constituent quark or antiquark may emit a virtual gluon which subsequently splits into quark q_3 and antiquark \bar{q}_4 . The three quarks and antiquarks then combine into mesons C_1 , C_2 , and C_3 . Four Feynman diagrams are shown in Fig. 1 for $A(q_1\bar{q}_1) + B(q_2\bar{q}_2) \rightarrow C_1(q_1\bar{q}_4) + C_2(q_2\bar{q}_1) + C_3(q_3\bar{q}_2)$, and four other diagrams in Fig. 2 for $A(q_1\bar{q}_1) + B(q_2\bar{q}_2) \rightarrow C_1(q_1\bar{q}_2) + C_2(q_2\bar{q}_4) + C_3(q_3\bar{q}_1)$. Diagram D₁ (D₂, D₃, D₄) in Fig. 1 involves the emission of a gluon from q_1 (\bar{q}_1 , q_2 , \bar{q}_2) and the subsequent splitting of the gluon into q_3 and \bar{q}_4 , and diagram D₅ (D₆, D₇, D₈) in Fig. 2 also involves this process. Denote the energy of meson A (B , C_1 , C_2 , C_3) by E_A (E_B , E_{C_1} , E_{C_2} , E_{C_3}). The total energy of the two initial mesons is $E_i = E_A + E_B$, and the total energy of the three final mesons is $E_f = E_{C_1} + E_{C_2} + E_{C_3}$. The S -matrix element for $A + B \rightarrow C_1 + C_2 + C_3$ is

$$\begin{aligned} S_{fi} &= \delta_{fi} - 2\pi i \delta(E_f - E_i) (< C_1, C_2, C_3 | V_{D_1} | A, B > + < C_1, C_2, C_3 | V_{D_2} | A, B > \\ &\quad + < C_1, C_2, C_3 | V_{D_3} | A, B > + < C_1, C_2, C_3 | V_{D_4} | A, B > \\ &\quad + < C_1, C_2, C_3 | V_{D_5} | A, B > + < C_1, C_2, C_3 | V_{D_6} | A, B > \\ &\quad + < C_1, C_2, C_3 | V_{D_7} | A, B > + < C_1, C_2, C_3 | V_{D_8} | A, B >), \end{aligned} \quad (1)$$

where V_{D_1} (V_{D_2} , V_{D_3} , V_{D_4}) represents the transition potential for $q_1 \rightarrow q_1 + q_3 + \bar{q}_4$ ($\bar{q}_1 \rightarrow$

$\bar{q}_1 + q_3 + \bar{q}_4$, $q_2 \rightarrow q_2 + q_3 + \bar{q}_4$, $\bar{q}_2 \rightarrow \bar{q}_2 + q_3 + \bar{q}_4$) in diagram D_1 (D_2 , D_3 , D_4), and V_{D_5} (V_{D_6} , V_{D_7} , V_{D_8}) represents the transition potential for $q_1 \rightarrow q_1 + q_3 + \bar{q}_4$ ($\bar{q}_1 \rightarrow \bar{q}_1 + q_3 + \bar{q}_4$, $q_2 \rightarrow q_2 + q_3 + \bar{q}_4$, $\bar{q}_2 \rightarrow \bar{q}_2 + q_3 + \bar{q}_4$) in diagram D_5 (D_6 , D_7 , D_8). Let \vec{P}_{ab} , \vec{R}_{ab} , and \vec{r}_{ab} be the total momentum, the center-of-mass coordinate, and the relative coordinate of constituents a and b , respectively. The wave function $|A, B\rangle$ of mesons A and B is

$$\psi_{q_1\bar{q}_1,q_2\bar{q}_2} = \frac{e^{i\vec{P}_{q_1\bar{q}_1}\cdot\vec{R}_{q_1\bar{q}_1}}}{\sqrt{V}}\psi_{q_1\bar{q}_1}(\vec{r}_{q_1\bar{q}_1})\frac{e^{i\vec{P}_{q_2\bar{q}_2}\cdot\vec{R}_{q_2\bar{q}_2}}}{\sqrt{V}}\psi_{q_2\bar{q}_2}(\vec{r}_{q_2\bar{q}_2}). \quad (2)$$

The wave function $|C_1, C_2, C_3\rangle$ of mesons C_1 , C_2 , and C_3 is

$$\psi_{q_1\bar{q}_4,q_2\bar{q}_1,q_3\bar{q}_2} = \frac{e^{i\vec{P}_{q_1\bar{q}_4}\cdot\vec{R}_{q_1\bar{q}_4}}}{\sqrt{V}}\psi_{q_1\bar{q}_4}(\vec{r}_{q_1\bar{q}_4})\frac{e^{i\vec{P}_{q_2\bar{q}_1}\cdot\vec{R}_{q_2\bar{q}_1}}}{\sqrt{V}}\psi_{q_2\bar{q}_1}(\vec{r}_{q_2\bar{q}_1})\frac{e^{i\vec{P}_{q_3\bar{q}_2}\cdot\vec{R}_{q_3\bar{q}_2}}}{\sqrt{V}}\psi_{q_3\bar{q}_2}(\vec{r}_{q_3\bar{q}_2}), \quad (3)$$

corresponding to the four diagrams in Fig. 1 or

$$\psi_{q_1\bar{q}_2,q_2\bar{q}_4,q_3\bar{q}_1} = \frac{e^{i\vec{P}_{q_1\bar{q}_2}\cdot\vec{R}_{q_1\bar{q}_2}}}{\sqrt{V}}\psi_{q_1\bar{q}_2}(\vec{r}_{q_1\bar{q}_2})\frac{e^{i\vec{P}_{q_2\bar{q}_4}\cdot\vec{R}_{q_2\bar{q}_4}}}{\sqrt{V}}\psi_{q_2\bar{q}_4}(\vec{r}_{q_2\bar{q}_4})\frac{e^{i\vec{P}_{q_3\bar{q}_1}\cdot\vec{R}_{q_3\bar{q}_1}}}{\sqrt{V}}\psi_{q_3\bar{q}_1}(\vec{r}_{q_3\bar{q}_1}), \quad (4)$$

corresponding to the four diagrams in Fig. 2. The mesonic quark-antiquark wave function $\psi_{ab}(\vec{r}_{ab})$ is the product of the color wave function, the spin wave function, the flavor wave function, and the relative-motion wave function of constituents a and b . Every meson wave function is normalized in the volume V .

From the S -matrix element we derive the transition amplitudes corresponding to the eight Feynman diagrams in Figs. 1 and 2. From the transition amplitudes we obtain the unpolarized cross section for $A + B \rightarrow C_1 + C_2 + C_3$. The position vector and the mass of constituent c are denoted by \vec{r}_c and m_c , respectively.

We first consider the four diagrams in Fig. 1. The five independent constituent position-vectors are \vec{r}_{q_1} , $\vec{r}_{\bar{q}_1}$, \vec{r}_{q_2} , $\vec{r}_{\bar{q}_2}$, and \vec{r}_{q_3} . They are related to the relative coordinates $(\vec{r}_{q_1\bar{q}_1}, \vec{r}_{q_2\bar{q}_2})$ and the center-of-mass coordinates $(\vec{R}_{q_1\bar{q}_4}, \vec{R}_{q_2\bar{q}_1}, \vec{R}_{q_3\bar{q}_2})$ by

$$\begin{aligned} \vec{r}_{q_1} &= \frac{m_{\bar{q}_1}m_{\bar{q}_2}m_{\bar{q}_4}}{m_{q_1}m_{q_2}m_{q_3} + m_{\bar{q}_1}m_{\bar{q}_2}m_{\bar{q}_4}}\vec{r}_{q_1\bar{q}_1} - \frac{m_{q_2}m_{\bar{q}_2}m_{\bar{q}_4}}{m_{q_1}m_{q_2}m_{q_3} + m_{\bar{q}_1}m_{\bar{q}_2}m_{\bar{q}_4}}\vec{r}_{q_2\bar{q}_2} \\ &+ \frac{m_{q_2}m_{q_3}(m_{q_1} + m_{\bar{q}_4})}{m_{q_1}m_{q_2}m_{q_3} + m_{\bar{q}_1}m_{\bar{q}_2}m_{\bar{q}_4}}\vec{R}_{q_1\bar{q}_4} + \frac{m_{\bar{q}_2}m_{\bar{q}_4}(m_{q_2} + m_{\bar{q}_1})}{m_{q_1}m_{q_2}m_{q_3} + m_{\bar{q}_1}m_{\bar{q}_2}m_{\bar{q}_4}}\vec{R}_{q_2\bar{q}_1} \\ &- \frac{m_{q_2}m_{\bar{q}_4}(m_{q_3} + m_{\bar{q}_2})}{m_{q_1}m_{q_2}m_{q_3} + m_{\bar{q}_1}m_{\bar{q}_2}m_{\bar{q}_4}}\vec{R}_{q_3\bar{q}_2}, \end{aligned} \quad (5)$$

$$\begin{aligned}
\vec{r}_{\bar{q}_1} &= -\frac{m_{q_1}m_{q_2}m_{q_3}}{m_{q_1}m_{q_2}m_{q_3} + m_{\bar{q}_1}m_{\bar{q}_2}m_{\bar{q}_4}}\vec{r}_{q_1\bar{q}_1} - \frac{m_{q_2}m_{\bar{q}_2}m_{\bar{q}_4}}{m_{q_1}m_{q_2}m_{q_3} + m_{\bar{q}_1}m_{\bar{q}_2}m_{\bar{q}_4}}\vec{r}_{q_2\bar{q}_2} \\
&+ \frac{m_{q_2}m_{q_3}(m_{q_1} + m_{\bar{q}_4})}{m_{q_1}m_{q_2}m_{q_3} + m_{\bar{q}_1}m_{\bar{q}_2}m_{\bar{q}_4}}\vec{R}_{q_1\bar{q}_4} + \frac{m_{\bar{q}_2}m_{\bar{q}_4}(m_{q_2} + m_{\bar{q}_1})}{m_{q_1}m_{q_2}m_{q_3} + m_{\bar{q}_1}m_{\bar{q}_2}m_{\bar{q}_4}}\vec{R}_{q_2\bar{q}_1} \\
&- \frac{m_{q_2}m_{\bar{q}_4}(m_{q_3} + m_{\bar{q}_2})}{m_{q_1}m_{q_2}m_{q_3} + m_{\bar{q}_1}m_{\bar{q}_2}m_{\bar{q}_4}}\vec{R}_{q_3\bar{q}_2},
\end{aligned} \tag{6}$$

$$\begin{aligned}
\vec{r}_{q_2} &= \frac{m_{q_1}m_{q_3}m_{\bar{q}_1}}{m_{q_1}m_{q_2}m_{q_3} + m_{\bar{q}_1}m_{\bar{q}_2}m_{\bar{q}_4}}\vec{r}_{q_1\bar{q}_1} + \frac{m_{\bar{q}_1}m_{\bar{q}_2}m_{\bar{q}_4}}{m_{q_1}m_{q_2}m_{q_3} + m_{\bar{q}_1}m_{\bar{q}_2}m_{\bar{q}_4}}\vec{r}_{q_2\bar{q}_2} \\
&- \frac{m_{q_3}m_{\bar{q}_1}(m_{q_1} + m_{\bar{q}_4})}{m_{q_1}m_{q_2}m_{q_3} + m_{\bar{q}_1}m_{\bar{q}_2}m_{\bar{q}_4}}\vec{R}_{q_1\bar{q}_4} + \frac{m_{q_1}m_{q_3}(m_{q_2} + m_{\bar{q}_1})}{m_{q_1}m_{q_2}m_{q_3} + m_{\bar{q}_1}m_{\bar{q}_2}m_{\bar{q}_4}}\vec{R}_{q_2\bar{q}_1} \\
&+ \frac{m_{\bar{q}_1}m_{\bar{q}_4}(m_{q_3} + m_{\bar{q}_2})}{m_{q_1}m_{q_2}m_{q_3} + m_{\bar{q}_1}m_{\bar{q}_2}m_{\bar{q}_4}}\vec{R}_{q_3\bar{q}_2},
\end{aligned} \tag{7}$$

$$\begin{aligned}
\vec{r}_{\bar{q}_2} &= \frac{m_{q_1}m_{q_3}m_{\bar{q}_1}}{m_{q_1}m_{q_2}m_{q_3} + m_{\bar{q}_1}m_{\bar{q}_2}m_{\bar{q}_4}}\vec{r}_{q_1\bar{q}_1} - \frac{m_{q_1}m_{q_2}m_{q_3}}{m_{q_1}m_{q_2}m_{q_3} + m_{\bar{q}_1}m_{\bar{q}_2}m_{\bar{q}_4}}\vec{r}_{q_2\bar{q}_2} \\
&- \frac{m_{q_3}m_{\bar{q}_1}(m_{q_1} + m_{\bar{q}_4})}{m_{q_1}m_{q_2}m_{q_3} + m_{\bar{q}_1}m_{\bar{q}_2}m_{\bar{q}_4}}\vec{R}_{q_1\bar{q}_4} + \frac{m_{q_1}m_{q_3}(m_{q_2} + m_{\bar{q}_1})}{m_{q_1}m_{q_2}m_{q_3} + m_{\bar{q}_1}m_{\bar{q}_2}m_{\bar{q}_4}}\vec{R}_{q_2\bar{q}_1} \\
&+ \frac{m_{\bar{q}_1}m_{\bar{q}_4}(m_{q_3} + m_{\bar{q}_2})}{m_{q_1}m_{q_2}m_{q_3} + m_{\bar{q}_1}m_{\bar{q}_2}m_{\bar{q}_4}}\vec{R}_{q_3\bar{q}_2},
\end{aligned} \tag{8}$$

$$\begin{aligned}
\vec{r}_{q_3} &= -\frac{m_{q_1}m_{\bar{q}_1}m_{\bar{q}_2}}{m_{q_1}m_{q_2}m_{q_3} + m_{\bar{q}_1}m_{\bar{q}_2}m_{\bar{q}_4}}\vec{r}_{q_1\bar{q}_1} + \frac{m_{q_1}m_{q_2}m_{\bar{q}_2}}{m_{q_1}m_{q_2}m_{q_3} + m_{\bar{q}_1}m_{\bar{q}_2}m_{\bar{q}_4}}\vec{r}_{q_2\bar{q}_2} \\
&+ \frac{m_{\bar{q}_1}m_{\bar{q}_2}(m_{q_1} + m_{\bar{q}_4})}{m_{q_1}m_{q_2}m_{q_3} + m_{\bar{q}_1}m_{\bar{q}_2}m_{\bar{q}_4}}\vec{R}_{q_1\bar{q}_4} - \frac{m_{q_1}m_{\bar{q}_2}(m_{q_2} + m_{\bar{q}_1})}{m_{q_1}m_{q_2}m_{q_3} + m_{\bar{q}_1}m_{\bar{q}_2}m_{\bar{q}_4}}\vec{R}_{q_2\bar{q}_1} \\
&+ \frac{m_{q_1}m_{q_2}(m_{q_3} + m_{\bar{q}_2})}{m_{q_1}m_{q_2}m_{q_3} + m_{\bar{q}_1}m_{\bar{q}_2}m_{\bar{q}_4}}\vec{R}_{q_3\bar{q}_2},
\end{aligned} \tag{9}$$

which lead to

$$\begin{aligned}
&d\vec{r}_{q_1}d\vec{r}_{\bar{q}_1}d\vec{r}_{q_2}d\vec{r}_{\bar{q}_2}d\vec{r}_{q_3} \\
&= \frac{(m_{q_1} + m_{\bar{q}_4})^3(m_{q_2} + m_{\bar{q}_1})^3(m_{q_3} + m_{\bar{q}_2})^3}{(m_{q_1}m_{q_2}m_{q_3} + m_{\bar{q}_1}m_{\bar{q}_2}m_{\bar{q}_4})^3}d\vec{r}_{q_1\bar{q}_1}d\vec{r}_{q_2\bar{q}_2}d\vec{R}_{q_1\bar{q}_4}d\vec{R}_{q_2\bar{q}_1}d\vec{R}_{q_3\bar{q}_2}.
\end{aligned} \tag{10}$$

Let \vec{R}_{total} be the center-of-mass coordinate of the initial or final mesons. Denote the three-dimensional momentum of meson A (B , C_1 , C_2 , C_3) by \vec{P}_A (\vec{P}_B , \vec{P}_{C_1} , \vec{P}_{C_2} , \vec{P}_{C_3}). The total momentum of the two initial mesons is $\vec{P}_i = \vec{P}_A + \vec{P}_B$, and the total momentum of the three final mesons is $\vec{P}_f = \vec{P}_{C_1} + \vec{P}_{C_2} + \vec{P}_{C_3}$. From the transition potential V_{D_1} and the wave functions of the initial and final mesons, we have for diagram D₁:

$$< C_1, C_2, C_3 | V_{D_1} | A, B >$$

$$\begin{aligned}
&= \langle q_1 \bar{q}_4, q_2 \bar{q}_1, q_3 \bar{q}_2 | V_{D_1} | q_1 \bar{q}_1, q_2 \bar{q}_2 \rangle \\
&= \int d\vec{r}_{q_1} d\vec{r}_{\bar{q}_1} d\vec{r}_{q_2} d\vec{r}_{\bar{q}_2} d\vec{r}_{q_3} \frac{e^{-i\vec{P}_{q_1 \bar{q}_4} \cdot \vec{R}_{q_1 \bar{q}_4}}}{\sqrt{V}} \psi_{q_1 \bar{q}_4}^+(\vec{r}_{q_1 \bar{q}_4}) \frac{e^{-i\vec{P}_{q_2 \bar{q}_1} \cdot \vec{R}_{q_2 \bar{q}_1}}}{\sqrt{V}} \psi_{q_2 \bar{q}_1}^+(\vec{r}_{q_2 \bar{q}_1}) \\
&\quad \frac{e^{-i\vec{P}_{q_3 \bar{q}_2} \cdot \vec{R}_{q_3 \bar{q}_2}}}{\sqrt{V}} \psi_{q_3 \bar{q}_2}^+(\vec{r}_{q_3 \bar{q}_2}) V_{D_1} \frac{e^{i\vec{P}_{q_1 \bar{q}_1} \cdot \vec{R}_{q_1 \bar{q}_1}}}{\sqrt{V}} \psi_{q_1 \bar{q}_1}(\vec{r}_{q_1 \bar{q}_1}) \frac{e^{i\vec{P}_{q_2 \bar{q}_2} \cdot \vec{R}_{q_2 \bar{q}_2}}}{\sqrt{V}} \psi_{q_2 \bar{q}_2}(\vec{r}_{q_2 \bar{q}_2}) \\
&= \frac{(m_{q_1} + m_{\bar{q}_4})^3 (m_{q_2} + m_{\bar{q}_1})^3 (m_{q_3} + m_{\bar{q}_2})^3}{\sqrt{V^5} (m_{q_1} m_{q_2} m_{q_3} + m_{\bar{q}_1} m_{\bar{q}_2} m_{\bar{q}_4})^3} \int d\vec{r}_{q_1 \bar{q}_1} d\vec{r}_{q_2 \bar{q}_2} d\vec{R}_{q_1 \bar{q}_4} d\vec{R}_{q_2 \bar{q}_1} d\vec{R}_{q_3 \bar{q}_2} \\
&\quad \psi_{q_1 \bar{q}_4}^+(\vec{r}_{q_1 \bar{q}_4}) \psi_{q_2 \bar{q}_1}^+(\vec{r}_{q_2 \bar{q}_1}) \psi_{q_3 \bar{q}_2}^+(\vec{r}_{q_3 \bar{q}_2}) V_{D_1} \psi_{q_1 \bar{q}_1}(\vec{r}_{q_1 \bar{q}_1}) \psi_{q_2 \bar{q}_2}(\vec{r}_{q_2 \bar{q}_2}) \\
&\quad \exp(-i\vec{P}_{q_1 \bar{q}_4} \cdot \vec{R}_{q_1 \bar{q}_4} - i\vec{P}_{q_2 \bar{q}_1} \cdot \vec{R}_{q_2 \bar{q}_1} - i\vec{P}_{q_3 \bar{q}_2} \cdot \vec{R}_{q_3 \bar{q}_2} + i\vec{P}_{q_1 \bar{q}_1} \cdot \vec{R}_{q_1 \bar{q}_1} + i\vec{P}_{q_2 \bar{q}_2} \cdot \vec{R}_{q_2 \bar{q}_2}),
\end{aligned} \tag{11}$$

where ψ_{ab}^+ is the Hermitean conjugate of ψ_{ab} . In the present work we limit ourselves to the case that at least two of the three final mesons have the same mass. We thus define the variable ρ_X from the position vectors of the two mesons with equal masses and the variable λ_X from the other meson. For example, supposing that mesons $C_1(q_1 \bar{q}_4)$ and $C_2(q_2 \bar{q}_1)$ have equal masses, we define

$$\rho_X = \frac{1}{\sqrt{2}}(\vec{R}_{q_1 \bar{q}_4} - \vec{R}_{q_2 \bar{q}_1}), \tag{12}$$

$$\lambda_X = \frac{1}{\sqrt{6}}(\vec{R}_{q_1 \bar{q}_4} + \vec{R}_{q_2 \bar{q}_1} - 2\vec{R}_{q_3 \bar{q}_2}), \tag{13}$$

which leads to

$$d\vec{R}_{q_1 \bar{q}_4} d\vec{R}_{q_2 \bar{q}_1} d\vec{R}_{q_3 \bar{q}_2} = 3\sqrt{3}d\vec{R}_{\text{total}} d\rho_X d\lambda_X. \tag{14}$$

From the mass m_{C_1} of meson C_1 , the mass m_{C_2} of meson C_2 , and the mass m_{C_3} of meson C_3 , we define

$$m_\rho = m_{C_1} = m_{C_2}, \tag{15}$$

$$m_\lambda = \frac{3m_{C_1} m_{C_3}}{2m_{C_1} + m_{C_3}}. \tag{16}$$

Let \vec{p}_{ρ_X} (\vec{p}_{λ_X}) be m_ρ (m_λ) times the derivative of ρ_X (λ_X) with respect to time. We then get

$$\vec{P}_{q_1 \bar{q}_4} \cdot \vec{R}_{q_1 \bar{q}_4} + \vec{P}_{q_2 \bar{q}_1} \cdot \vec{R}_{q_2 \bar{q}_1} + \vec{P}_{q_3 \bar{q}_2} \cdot \vec{R}_{q_3 \bar{q}_2} = \vec{P}_f \cdot \vec{R}_{\text{total}} + \vec{p}_{\rho_X} \cdot \rho_X + \vec{p}_{\lambda_X} \cdot \lambda_X. \tag{17}$$

In terms of ρ_X , λ_X , \vec{p}_{ρ_X} , and \vec{p}_{λ_X} , we have

$$\langle C_1, C_2, C_3 | V_{D_1} | A, B \rangle$$

$$\begin{aligned}
&= \frac{3\sqrt{3}(m_{q_1} + m_{\bar{q}_4})^3(m_{q_2} + m_{\bar{q}_1})^3(m_{q_3} + m_{\bar{q}_2})^3}{\sqrt{V^5}(m_{q_1}m_{q_2}m_{q_3} + m_{\bar{q}_1}m_{\bar{q}_2}m_{\bar{q}_4})^3} \int d\vec{r}_{q_1\bar{q}_1} d\vec{r}_{q_2\bar{q}_2} d\vec{R}_{\text{total}} d\vec{\rho}_X d\vec{\lambda}_X \\
&\quad \psi_{q_1\bar{q}_4}^+(\vec{r}_{q_1\bar{q}_4}) \psi_{q_2\bar{q}_1}^+(\vec{r}_{q_2\bar{q}_1}) \psi_{q_3\bar{q}_2}^+(\vec{r}_{q_3\bar{q}_2}) V_{D_1} \psi_{q_1\bar{q}_1}(\vec{r}_{q_1\bar{q}_1}) \psi_{q_2\bar{q}_2}(\vec{r}_{q_2\bar{q}_2}) \\
&\quad \exp(-i\vec{P}_f \cdot \vec{R}_{\text{total}} - i\vec{p}_{\rho_X} \cdot \vec{\rho}_X - i\vec{p}_{\lambda_X} \cdot \vec{\lambda}_X + i\vec{P}_i \cdot \vec{R}_{\text{total}} + i\vec{p}_{q_1\bar{q}_1, q_2\bar{q}_2} \cdot \vec{r}_{q_1\bar{q}_1, q_2\bar{q}_2}) \\
&= (2\pi)^3 \delta^3(\vec{P}_i - \vec{P}_f) \frac{\mathcal{M}_{D_1}}{\sqrt{V^5} \sqrt{2E_A 2E_B 2E_{C_1} 2E_{C_2} 2E_{C_3}}}, \tag{18}
\end{aligned}$$

where $\vec{r}_{q_1\bar{q}_1, q_2\bar{q}_2}$ and $\vec{p}_{q_1\bar{q}_1, q_2\bar{q}_2}$ are the relative coordinate and the relative momentum of $q_1\bar{q}_1$ and $q_2\bar{q}_2$, respectively. \mathcal{M}_{D_1} is the transition amplitude given by

$$\begin{aligned}
\mathcal{M}_{D_1} &= \sqrt{2E_A 2E_B 2E_{C_1} 2E_{C_2} 2E_{C_3}} \frac{3\sqrt{3}(m_{q_1} + m_{\bar{q}_4})^3(m_{q_2} + m_{\bar{q}_1})^3(m_{q_3} + m_{\bar{q}_2})^3}{(m_{q_1}m_{q_2}m_{q_3} + m_{\bar{q}_1}m_{\bar{q}_2}m_{\bar{q}_4})^3} \\
&\quad \int d\vec{r}_{q_1\bar{q}_1} d\vec{r}_{q_2\bar{q}_2} d\vec{\rho}_X d\vec{\lambda}_X \psi_{q_1\bar{q}_4}^+(\vec{r}_{q_1\bar{q}_4}) \psi_{q_2\bar{q}_1}^+(\vec{r}_{q_2\bar{q}_1}) \psi_{q_3\bar{q}_2}^+(\vec{r}_{q_3\bar{q}_2}) V_{D_1} \\
&\quad \psi_{q_1\bar{q}_1}(\vec{r}_{q_1\bar{q}_1}) \psi_{q_2\bar{q}_2}(\vec{r}_{q_2\bar{q}_2}) \exp(-i\vec{p}_{\rho_X} \cdot \vec{\rho}_X - i\vec{p}_{\lambda_X} \cdot \vec{\lambda}_X + i\vec{p}_{q_1\bar{q}_1, q_2\bar{q}_2} \cdot \vec{r}_{q_1\bar{q}_1, q_2\bar{q}_2}). \tag{19}
\end{aligned}$$

For diagram D₂ we have

$$\begin{aligned}
\langle C_1, C_2, C_3 | V_{D_2} | A, B \rangle &= \langle q_1\bar{q}_4, q_2\bar{q}_1, q_3\bar{q}_2 | V_{D_2} | q_1\bar{q}_1, q_2\bar{q}_2 \rangle \\
&= (2\pi)^3 \delta^3(\vec{P}_i - \vec{P}_f) \frac{\mathcal{M}_{D_2}}{\sqrt{V^5} \sqrt{2E_A 2E_B 2E_{C_1} 2E_{C_2} 2E_{C_3}}}, \tag{20}
\end{aligned}$$

where the transition amplitude \mathcal{M}_{D_2} is obtained from Eq. (19) by replacing V_{D_1} with V_{D_2} . For diagram D₃ we have

$$\begin{aligned}
\langle C_1, C_2, C_3 | V_{D_3} | A, B \rangle &= \langle q_1\bar{q}_4, q_2\bar{q}_1, q_3\bar{q}_2 | V_{D_3} | q_1\bar{q}_1, q_2\bar{q}_2 \rangle \\
&= (2\pi)^3 \delta^3(\vec{P}_i - \vec{P}_f) \frac{\mathcal{M}_{D_3}}{\sqrt{V^5} \sqrt{2E_A 2E_B 2E_{C_1} 2E_{C_2} 2E_{C_3}}}, \tag{21}
\end{aligned}$$

where the transition amplitude \mathcal{M}_{D_3} is obtained from Eq. (19) by replacing V_{D_1} with V_{D_3} . For diagram D₄ we have

$$\begin{aligned}
\langle C_1, C_2, C_3 | V_{D_4} | A, B \rangle &= \langle q_1\bar{q}_4, q_2\bar{q}_1, q_3\bar{q}_2 | V_{D_4} | q_1\bar{q}_1, q_2\bar{q}_2 \rangle \\
&= (2\pi)^3 \delta^3(\vec{P}_i - \vec{P}_f) \frac{\mathcal{M}_{D_4}}{\sqrt{V^5} \sqrt{2E_A 2E_B 2E_{C_1} 2E_{C_2} 2E_{C_3}}}, \tag{22}
\end{aligned}$$

where the transition amplitude \mathcal{M}_{D_4} is obtained from Eq. (19) by replacing V_{D_1} with V_{D_4} .

Next, we consider the four diagrams in Fig. 2. The five independent constituent position-vectors, \vec{r}_{q_1} , $\vec{r}_{\bar{q}_1}$, \vec{r}_{q_2} , $\vec{r}_{\bar{q}_2}$, and \vec{r}_{q_3} , are related to $\vec{r}_{q_1\bar{q}_1}$, $\vec{r}_{q_2\bar{q}_2}$, $\vec{R}_{q_1\bar{q}_2}$, $\vec{R}_{q_2\bar{q}_4}$, and $\vec{R}_{q_3\bar{q}_1}$ by

$$\begin{aligned}\vec{r}_{q_1} &= \frac{m_{\bar{q}_1}m_{\bar{q}_2}m_{\bar{q}_4}}{m_{q_1}m_{q_2}m_{q_3} + m_{\bar{q}_1}m_{\bar{q}_2}m_{\bar{q}_4}}\vec{r}_{q_1\bar{q}_1} + \frac{m_{q_2}m_{q_3}m_{\bar{q}_2}}{m_{q_1}m_{q_2}m_{q_3} + m_{\bar{q}_1}m_{\bar{q}_2}m_{\bar{q}_4}}\vec{r}_{q_2\bar{q}_2} \\ &+ \frac{m_{q_2}m_{q_3}(m_{q_1} + m_{\bar{q}_2})}{m_{q_1}m_{q_2}m_{q_3} + m_{\bar{q}_1}m_{\bar{q}_2}m_{\bar{q}_4}}\vec{R}_{q_1\bar{q}_2} - \frac{m_{q_3}m_{\bar{q}_2}(m_{q_2} + m_{\bar{q}_4})}{m_{q_1}m_{q_2}m_{q_3} + m_{\bar{q}_1}m_{\bar{q}_2}m_{\bar{q}_4}}\vec{R}_{q_2\bar{q}_4} \\ &+ \frac{m_{\bar{q}_2}m_{\bar{q}_4}(m_{q_3} + m_{\bar{q}_1})}{m_{q_1}m_{q_2}m_{q_3} + m_{\bar{q}_1}m_{\bar{q}_2}m_{\bar{q}_4}}\vec{R}_{q_3\bar{q}_1},\end{aligned}\tag{23}$$

$$\begin{aligned}\vec{r}_{\bar{q}_1} &= -\frac{m_{q_1}m_{q_2}m_{q_3}}{m_{q_1}m_{q_2}m_{q_3} + m_{\bar{q}_1}m_{\bar{q}_2}m_{\bar{q}_4}}\vec{r}_{q_1\bar{q}_1} + \frac{m_{q_2}m_{q_3}m_{\bar{q}_2}}{m_{q_1}m_{q_2}m_{q_3} + m_{\bar{q}_1}m_{\bar{q}_2}m_{\bar{q}_4}}\vec{r}_{q_2\bar{q}_2} \\ &+ \frac{m_{q_2}m_{q_3}(m_{q_1} + m_{\bar{q}_2})}{m_{q_1}m_{q_2}m_{q_3} + m_{\bar{q}_1}m_{\bar{q}_2}m_{\bar{q}_4}}\vec{R}_{q_1\bar{q}_2} - \frac{m_{q_3}m_{\bar{q}_2}(m_{q_2} + m_{\bar{q}_4})}{m_{q_1}m_{q_2}m_{q_3} + m_{\bar{q}_1}m_{\bar{q}_2}m_{\bar{q}_4}}\vec{R}_{q_2\bar{q}_4} \\ &+ \frac{m_{\bar{q}_2}m_{\bar{q}_4}(m_{q_3} + m_{\bar{q}_1})}{m_{q_1}m_{q_2}m_{q_3} + m_{\bar{q}_1}m_{\bar{q}_2}m_{\bar{q}_4}}\vec{R}_{q_3\bar{q}_1},\end{aligned}\tag{24}$$

$$\begin{aligned}\vec{r}_{q_2} &= -\frac{m_{q_1}m_{\bar{q}_1}m_{\bar{q}_4}}{m_{q_1}m_{q_2}m_{q_3} + m_{\bar{q}_1}m_{\bar{q}_2}m_{\bar{q}_4}}\vec{r}_{q_1\bar{q}_1} + \frac{m_{\bar{q}_1}m_{\bar{q}_2}m_{\bar{q}_4}}{m_{q_1}m_{q_2}m_{q_3} + m_{\bar{q}_1}m_{\bar{q}_2}m_{\bar{q}_4}}\vec{r}_{q_2\bar{q}_2} \\ &+ \frac{m_{\bar{q}_1}m_{\bar{q}_4}(m_{q_1} + m_{\bar{q}_2})}{m_{q_1}m_{q_2}m_{q_3} + m_{\bar{q}_1}m_{\bar{q}_2}m_{\bar{q}_4}}\vec{R}_{q_1\bar{q}_2} + \frac{m_{q_1}m_{q_3}(m_{q_2} + m_{\bar{q}_4})}{m_{q_1}m_{q_2}m_{q_3} + m_{\bar{q}_1}m_{\bar{q}_2}m_{\bar{q}_4}}\vec{R}_{q_2\bar{q}_4} \\ &- \frac{m_{q_1}m_{\bar{q}_4}(m_{q_3} + m_{\bar{q}_1})}{m_{q_1}m_{q_2}m_{q_3} + m_{\bar{q}_1}m_{\bar{q}_2}m_{\bar{q}_4}}\vec{R}_{q_3\bar{q}_1},\end{aligned}\tag{25}$$

$$\begin{aligned}\vec{r}_{\bar{q}_2} &= -\frac{m_{q_1}m_{\bar{q}_1}m_{\bar{q}_4}}{m_{q_1}m_{q_2}m_{q_3} + m_{\bar{q}_1}m_{\bar{q}_2}m_{\bar{q}_4}}\vec{r}_{q_1\bar{q}_1} - \frac{m_{q_1}m_{q_2}m_{q_3}}{m_{q_1}m_{q_2}m_{q_3} + m_{\bar{q}_1}m_{\bar{q}_2}m_{\bar{q}_4}}\vec{r}_{q_2\bar{q}_2} \\ &+ \frac{m_{\bar{q}_1}m_{\bar{q}_4}(m_{q_1} + m_{\bar{q}_2})}{m_{q_1}m_{q_2}m_{q_3} + m_{\bar{q}_1}m_{\bar{q}_2}m_{\bar{q}_4}}\vec{R}_{q_1\bar{q}_2} + \frac{m_{q_1}m_{q_3}(m_{q_2} + m_{\bar{q}_4})}{m_{q_1}m_{q_2}m_{q_3} + m_{\bar{q}_1}m_{\bar{q}_2}m_{\bar{q}_4}}\vec{R}_{q_2\bar{q}_4} \\ &- \frac{m_{q_1}m_{\bar{q}_4}(m_{q_3} + m_{\bar{q}_1})}{m_{q_1}m_{q_2}m_{q_3} + m_{\bar{q}_1}m_{\bar{q}_2}m_{\bar{q}_4}}\vec{R}_{q_3\bar{q}_1},\end{aligned}\tag{26}$$

$$\begin{aligned}\vec{r}_{q_3} &= \frac{m_{q_1}m_{q_2}m_{\bar{q}_1}}{m_{q_1}m_{q_2}m_{q_3} + m_{\bar{q}_1}m_{\bar{q}_2}m_{\bar{q}_4}}\vec{r}_{q_1\bar{q}_1} - \frac{m_{q_2}m_{\bar{q}_1}m_{\bar{q}_2}}{m_{q_1}m_{q_2}m_{q_3} + m_{\bar{q}_1}m_{\bar{q}_2}m_{\bar{q}_4}}\vec{r}_{q_2\bar{q}_2} \\ &- \frac{m_{q_2}m_{\bar{q}_1}(m_{q_1} + m_{\bar{q}_2})}{m_{q_1}m_{q_2}m_{q_3} + m_{\bar{q}_1}m_{\bar{q}_2}m_{\bar{q}_4}}\vec{R}_{q_1\bar{q}_2} + \frac{m_{\bar{q}_1}m_{\bar{q}_2}(m_{q_2} + m_{\bar{q}_4})}{m_{q_1}m_{q_2}m_{q_3} + m_{\bar{q}_1}m_{\bar{q}_2}m_{\bar{q}_4}}\vec{R}_{q_2\bar{q}_4} \\ &+ \frac{m_{q_1}m_{q_2}(m_{q_3} + m_{\bar{q}_1})}{m_{q_1}m_{q_2}m_{q_3} + m_{\bar{q}_1}m_{\bar{q}_2}m_{\bar{q}_4}}\vec{R}_{q_3\bar{q}_1},\end{aligned}\tag{27}$$

which lead to

$$d\vec{r}_{q_1}d\vec{r}_{\bar{q}_1}d\vec{r}_{q_2}d\vec{r}_{\bar{q}_2}d\vec{r}_{q_3}$$

$$= \frac{(m_{q_1} + m_{\bar{q}_2})^3 (m_{q_2} + m_{\bar{q}_4})^3 (m_{q_3} + m_{\bar{q}_1})^3}{(m_{q_1} m_{q_2} m_{q_3} + m_{\bar{q}_1} m_{\bar{q}_2} m_{\bar{q}_4})^3} d\vec{r}_{q_1\bar{q}_1} d\vec{r}_{q_2\bar{q}_2} d\vec{R}_{q_1\bar{q}_2} d\vec{R}_{q_2\bar{q}_4} d\vec{R}_{q_3\bar{q}_1}. \quad (28)$$

From the transition potential V_{D_5} and the wave functions of the initial and final mesons, we have for diagram D_5 in Fig. 2:

$$\begin{aligned} & \langle C_1, C_2, C_3 | V_{D_5} | A, B \rangle \\ &= \langle q_1\bar{q}_2, q_2\bar{q}_4, q_3\bar{q}_1 | V_{D_5} | q_1\bar{q}_1, q_2\bar{q}_2 \rangle \\ &= \int d\vec{r}_{q_1} d\vec{r}_{\bar{q}_1} d\vec{r}_{q_2} d\vec{r}_{\bar{q}_2} d\vec{r}_{q_3} \frac{e^{-i\vec{P}_{q_1\bar{q}_2}\cdot\vec{R}_{q_1\bar{q}_2}}}{\sqrt{V}} \psi_{q_1\bar{q}_2}^+(\vec{r}_{q_1\bar{q}_2}) \frac{e^{-i\vec{P}_{q_2\bar{q}_4}\cdot\vec{R}_{q_2\bar{q}_4}}}{\sqrt{V}} \psi_{q_2\bar{q}_4}^+(\vec{r}_{q_2\bar{q}_4}) \\ &\quad \frac{e^{-i\vec{P}_{q_3\bar{q}_1}\cdot\vec{R}_{q_3\bar{q}_1}}}{\sqrt{V}} \psi_{q_3\bar{q}_1}^+(\vec{r}_{q_3\bar{q}_1}) V_{D_5} \frac{e^{i\vec{P}_{q_1\bar{q}_1}\cdot\vec{R}_{q_1\bar{q}_1}}}{\sqrt{V}} \psi_{q_1\bar{q}_1}(\vec{r}_{q_1\bar{q}_1}) \frac{e^{i\vec{P}_{q_2\bar{q}_2}\cdot\vec{R}_{q_2\bar{q}_2}}}{\sqrt{V}} \psi_{q_2\bar{q}_2}(\vec{r}_{q_2\bar{q}_2}) \\ &= \frac{(m_{q_1} + m_{\bar{q}_2})^3 (m_{q_2} + m_{\bar{q}_4})^3 (m_{q_3} + m_{\bar{q}_1})^3}{\sqrt{V^5} (m_{q_1} m_{q_2} m_{q_3} + m_{\bar{q}_1} m_{\bar{q}_2} m_{\bar{q}_4})^3} \int d\vec{r}_{q_1\bar{q}_1} d\vec{r}_{q_2\bar{q}_2} d\vec{R}_{q_1\bar{q}_2} d\vec{R}_{q_2\bar{q}_4} d\vec{R}_{q_3\bar{q}_1} \\ &\quad \psi_{q_1\bar{q}_2}^+(\vec{r}_{q_1\bar{q}_2}) \psi_{q_2\bar{q}_4}^+(\vec{r}_{q_2\bar{q}_4}) \psi_{q_3\bar{q}_1}^+(\vec{r}_{q_3\bar{q}_1}) V_{D_5} \psi_{q_1\bar{q}_1}(\vec{r}_{q_1\bar{q}_1}) \psi_{q_2\bar{q}_2}(\vec{r}_{q_2\bar{q}_2}) \\ &\quad \exp(-i\vec{P}_{q_1\bar{q}_2}\cdot\vec{R}_{q_1\bar{q}_2} - i\vec{P}_{q_2\bar{q}_4}\cdot\vec{R}_{q_2\bar{q}_4} - i\vec{P}_{q_3\bar{q}_1}\cdot\vec{R}_{q_3\bar{q}_1} + i\vec{P}_{q_1\bar{q}_1}\cdot\vec{R}_{q_1\bar{q}_1} + i\vec{P}_{q_2\bar{q}_2}\cdot\vec{R}_{q_2\bar{q}_2}) \\ &= \frac{3\sqrt{3}(m_{q_1} + m_{\bar{q}_2})^3 (m_{q_2} + m_{\bar{q}_4})^3 (m_{q_3} + m_{\bar{q}_1})^3}{\sqrt{V^5} (m_{q_1} m_{q_2} m_{q_3} + m_{\bar{q}_1} m_{\bar{q}_2} m_{\bar{q}_4})^3} \int d\vec{r}_{q_1\bar{q}_1} d\vec{r}_{q_2\bar{q}_2} d\vec{R}_{\text{total}} d\vec{\rho}_Y d\vec{\lambda}_Y \\ &\quad \psi_{q_1\bar{q}_2}^+(\vec{r}_{q_1\bar{q}_2}) \psi_{q_2\bar{q}_4}^+(\vec{r}_{q_2\bar{q}_4}) \psi_{q_3\bar{q}_1}^+(\vec{r}_{q_3\bar{q}_1}) V_{D_5} \psi_{q_1\bar{q}_1}(\vec{r}_{q_1\bar{q}_1}) \psi_{q_2\bar{q}_2}(\vec{r}_{q_2\bar{q}_2}) \\ &\quad \exp(-i\vec{P}_f\cdot\vec{R}_{\text{total}} - i\vec{p}_{\rho_Y}\cdot\vec{\rho}_Y - i\vec{p}_{\lambda_Y}\cdot\vec{\lambda}_Y + i\vec{P}_i\cdot\vec{R}_{\text{total}} + i\vec{p}_{q_1\bar{q}_1, q_2\bar{q}_2}\cdot\vec{r}_{q_1\bar{q}_1, q_2\bar{q}_2}) \\ &= (2\pi)^3 \delta^3(\vec{P}_i - \vec{P}_f) \frac{\mathcal{M}_{D_5}}{\sqrt{V^5} \sqrt{2E_A 2E_B 2E_{C_1} 2E_{C_2} 2E_{C_3}}}, \end{aligned} \quad (29)$$

where \mathcal{M}_{D_5} is the transition amplitude given by

$$\begin{aligned} \mathcal{M}_{D_5} &= \sqrt{2E_A 2E_B 2E_{C_1} 2E_{C_2} 2E_{C_3}} \frac{3\sqrt{3}(m_{q_1} + m_{\bar{q}_2})^3 (m_{q_2} + m_{\bar{q}_4})^3 (m_{q_3} + m_{\bar{q}_1})^3}{(m_{q_1} m_{q_2} m_{q_3} + m_{\bar{q}_1} m_{\bar{q}_2} m_{\bar{q}_4})^3} \\ &\quad \int d\vec{r}_{q_1\bar{q}_1} d\vec{r}_{q_2\bar{q}_2} d\vec{\rho}_Y d\vec{\lambda}_Y \psi_{q_1\bar{q}_2}^+(\vec{r}_{q_1\bar{q}_2}) \psi_{q_2\bar{q}_4}^+(\vec{r}_{q_2\bar{q}_4}) \psi_{q_3\bar{q}_1}^+(\vec{r}_{q_3\bar{q}_1}) V_{D_5} \\ &\quad \psi_{q_1\bar{q}_1}(\vec{r}_{q_1\bar{q}_1}) \psi_{q_2\bar{q}_2}(\vec{r}_{q_2\bar{q}_2}) \exp(-i\vec{p}_{\rho_Y}\cdot\vec{\rho}_Y - i\vec{p}_{\lambda_Y}\cdot\vec{\lambda}_Y + i\vec{p}_{q_1\bar{q}_1, q_2\bar{q}_2}\cdot\vec{r}_{q_1\bar{q}_1, q_2\bar{q}_2}). \end{aligned} \quad (30)$$

In the above two equations the variable $\vec{\rho}_Y$ is defined from the position vectors of the two mesons with equal masses, and the variable $\vec{\lambda}_Y$ from the other meson. In case that mesons $C_1(q_1\bar{q}_2)$ and $C_2(q_2\bar{q}_4)$ have the same mass, we define

$$\vec{\rho}_Y = \frac{1}{\sqrt{2}}(\vec{R}_{q_1\bar{q}_2} - \vec{R}_{q_2\bar{q}_4}), \quad (31)$$

$$\vec{\lambda}_Y = \frac{1}{\sqrt{6}}(\vec{R}_{q_1\bar{q}_2} + \vec{R}_{q_2\bar{q}_4} - 2\vec{R}_{q_3\bar{q}_1}). \quad (32)$$

Let \vec{p}_{ρ_Y} (\vec{p}_{λ_Y}) be m_ρ (m_λ) times the derivative of $\vec{\rho}_Y$ ($\vec{\lambda}_Y$) with respect to time. In Eq. (29) we have used the two equalities,

$$d\vec{R}_{q_1\bar{q}_2} d\vec{R}_{q_2\bar{q}_4} d\vec{R}_{q_3\bar{q}_1} = 3\sqrt{3}d\vec{R}_{\text{total}} d\vec{\rho}_Y d\vec{\lambda}_Y, \quad (33)$$

$$\vec{P}_{q_1\bar{q}_2} \cdot \vec{R}_{q_1\bar{q}_2} + \vec{P}_{q_2\bar{q}_4} \cdot \vec{R}_{q_2\bar{q}_4} + \vec{P}_{q_3\bar{q}_1} \cdot \vec{R}_{q_3\bar{q}_1} = \vec{P}_f \cdot \vec{R}_{\text{total}} + \vec{p}_{\rho_Y} \cdot \vec{\rho}_Y + \vec{p}_{\lambda_Y} \cdot \vec{\lambda}_Y. \quad (34)$$

For diagram D₆ we have

$$\begin{aligned} < C_1, C_2, C_3 | V_{D_6} | A, B > &= < q_1\bar{q}_2, q_2\bar{q}_4, q_3\bar{q}_1 | V_{D_6} | q_1\bar{q}_1, q_2\bar{q}_2 > \\ &= (2\pi)^3 \delta^3(\vec{P}_i - \vec{P}_f) \frac{\mathcal{M}_{D_6}}{\sqrt{V^5} \sqrt{2E_A 2E_B 2E_{C_1} 2E_{C_2} 2E_{C_3}}}, \end{aligned} \quad (35)$$

where the transition amplitude \mathcal{M}_{D_6} is obtained from Eq. (30) by replacing V_{D_5} with V_{D_6} . For diagram D₇ we have

$$\begin{aligned} < C_1, C_2, C_3 | V_{D_7} | A, B > &= < q_1\bar{q}_2, q_2\bar{q}_4, q_3\bar{q}_1 | V_{D_7} | q_1\bar{q}_1, q_2\bar{q}_2 > \\ &= (2\pi)^3 \delta^3(\vec{P}_i - \vec{P}_f) \frac{\mathcal{M}_{D_7}}{\sqrt{V^5} \sqrt{2E_A 2E_B 2E_{C_1} 2E_{C_2} 2E_{C_3}}}, \end{aligned} \quad (36)$$

where the transition amplitude \mathcal{M}_{D_7} is obtained from Eq. (30) by replacing V_{D_5} with V_{D_7} . For diagram D₈ we have

$$\begin{aligned} < C_1, C_2, C_3 | V_{D_8} | A, B > &= < q_1\bar{q}_2, q_2\bar{q}_4, q_3\bar{q}_1 | V_{D_8} | q_1\bar{q}_1, q_2\bar{q}_2 > \\ &= (2\pi)^3 \delta^3(\vec{P}_i - \vec{P}_f) \frac{\mathcal{M}_{D_8}}{\sqrt{V^5} \sqrt{2E_A 2E_B 2E_{C_1} 2E_{C_2} 2E_{C_3}}}, \end{aligned} \quad (37)$$

where the transition amplitude \mathcal{M}_{D_8} is obtained from Eq. (30) by replacing V_{D_5} with V_{D_8} .

Let P_A (P_B) and m_A (m_B) be the four-momentum and the mass of meson A (B), respectively, and we have the Mandelstam variable $s = (P_A + P_B)^2$. Along the general lines provided in Ref. [59] on deriving the cross section from the transition amplitude, we get the unpolarized cross section for $A + B \rightarrow C_1 + C_2 + C_3$,

$$\begin{aligned} \sigma^{\text{unpol}} &= \frac{(2\pi)^4}{4\sqrt{(P_A \cdot P_B)^2 - m_A^2 m_B^2}} \frac{1}{(2J_A + 1)(2J_B + 1)} \\ &\quad \int \frac{d^3 P_{C_1}}{(2\pi)^3 2E_{C_1}} \frac{d^3 P_{C_2}}{(2\pi)^3 2E_{C_2}} \frac{d^3 P_{C_3}}{(2\pi)^3 2E_{C_3}} \delta(E_f - E_i) \delta^3(\vec{P}_f - \vec{P}_i) \end{aligned}$$

$$\sum_{J_{Az}J_{Bz}J_{C_1z}J_{C_2z}J_{C_3z}} |\mathcal{M}_{D_1} + \mathcal{M}_{D_2} + \mathcal{M}_{D_3} + \mathcal{M}_{D_4} + \mathcal{M}_{D_5} + \mathcal{M}_{D_6} + \mathcal{M}_{D_7} + \mathcal{M}_{D_8}|^2, \quad (38)$$

where J_i ($i = A, B, C_1, C_2, C_3$) is the angular momentum of meson i with the magnetic projection quantum number J_{iz} . With the equality $(P_A \cdot P_B)^2 - m_A^2 m_B^2 = 0.25[s - (m_A + m_B)^2][s - (m_A - m_B)^2]$, integration over \vec{P}_{C_2} leads to

$$\begin{aligned} \sigma^{\text{unpol}} = & \frac{1}{16(2\pi)^5 \sqrt{[s - (m_A + m_B)^2][s - (m_A - m_B)^2]}} \frac{1}{(2J_A + 1)(2J_B + 1)} \\ & \int \frac{d^3 P_{C_1} d^3 P_{C_3}}{E_{C_1} E_{C_2} E_{C_3}} \delta(E_f - E_i) \sum_{J_{Az}J_{Bz}J_{C_1z}J_{C_2z}J_{C_3z}} |\mathcal{M}_{D_1} + \mathcal{M}_{D_2} \\ & + \mathcal{M}_{D_3} + \mathcal{M}_{D_4} + \mathcal{M}_{D_5} + \mathcal{M}_{D_6} + \mathcal{M}_{D_7} + \mathcal{M}_{D_8}|^2. \end{aligned} \quad (39)$$

Integration over $|\vec{P}_{C_1}|$ yields

$$\begin{aligned} \sigma^{\text{unpol}} = & \frac{1}{16(2\pi)^5 \sqrt{[s - (m_A + m_B)^2][s - (m_A - m_B)^2]}} \frac{1}{(2J_A + 1)(2J_B + 1)} \\ & \int \frac{d^3 P_{C_3} d\Omega_{C_1}}{E_{C_3}} \frac{|\vec{P}_{C_1}|_0^2}{||\vec{P}_{C_1}|_0 E_{C_2} + (|\vec{P}_{C_1}|_0 - |\vec{P}_A + \vec{P}_B - \vec{P}_{C_3}| \cos \Theta) E_{C_1}|} \\ & \sum_{J_{Az}J_{Bz}J_{C_1z}J_{C_2z}J_{C_3z}} |\mathcal{M}_{D_1} + \mathcal{M}_{D_2} + \mathcal{M}_{D_3} + \mathcal{M}_{D_4} + \mathcal{M}_{D_5} + \mathcal{M}_{D_6} \\ & + \mathcal{M}_{D_7} + \mathcal{M}_{D_8}|^2, \end{aligned} \quad (40)$$

where Θ is the angle between \vec{P}_{C_1} and $\vec{P}_A + \vec{P}_B - \vec{P}_{C_3}$, $d\Omega_{C_1}$ is the solid angle centered about the direction of \vec{P}_{C_1} , and $|\vec{P}_{C_1}|_0$ is the absolute value of \vec{P}_{C_1} that satisfies $E_f - E_i = 0$. The unpolarized cross section is a function of \sqrt{s} , which is the total energy of the two initial mesons in the center-of-mass frame.

III. TRANSITION POTENTIAL

In Fig. 3 the left diagram denotes the process $q'(p_1) \rightarrow q'(p'_1) + q(p_3) + \bar{q}(-p_4)$, and the right diagram $\bar{q}'(-p_1) \rightarrow \bar{q}'(-p'_1) + q(p_3) + \bar{q}(-p_4)$. In each diagram the wavy line represents the gluon which has four-momentum k , the color index e , and the space-time index τ . Each vertex involves the gauge coupling constant g_s , the $SU(3)$ color generators T^e ($e = 1, \dots, 8$), and the Dirac matrices γ^τ . According to the Feynman rules in QCD [60],

the amplitude for the left diagram in Fig. 3 is written as

$$\mathcal{M}_{cq'q\bar{q}} = \frac{g_s^2}{k^2} \bar{\psi}_{q'}(\vec{p}_1', s_{q'z}) \gamma_\tau T^e \psi_{q'}(\vec{p}_1, s_{q'z}) \bar{\psi}_q(\vec{p}_3, s_{qz}) \gamma^\tau T^e \psi_{\bar{q}}(\vec{p}_4, s_{\bar{q}z}), \quad (41)$$

and the amplitude for the right diagram is

$$\mathcal{M}_{c\bar{q}'q\bar{q}} = -\frac{g_s^2}{k^2} \bar{\psi}_{\bar{q}'}(\vec{p}_1, s_{\bar{q}'z}) \gamma_\tau T^e \psi_{\bar{q}'}(\vec{p}_1', s_{\bar{q}'z}) \bar{\psi}_q(\vec{p}_3, s_{qz}) \gamma^\tau T^e \psi_{\bar{q}}(\vec{p}_4, s_{\bar{q}z}), \quad (42)$$

where repeated color and space-time indices (e and τ) are summed. The quark spinors ($\psi_{q'}(\vec{p}_1, s_{q'z})$, $\psi_{q'}(\vec{p}_1', s_{q'z})$, $\psi_q(\vec{p}_3, s_{qz})$) and the antiquark spinors ($\psi_{\bar{q}}(\vec{p}_4, s_{\bar{q}z})$, $\psi_{\bar{q}'}(\vec{p}_1, s_{\bar{q}'z})$, $\psi_{\bar{q}'}(\vec{p}_1', s_{\bar{q}'z})$) are given by [53, 59]

$$\psi_q(\vec{p}_3, s_{qz}) = \begin{pmatrix} G_3(\vec{p}_3) \\ \frac{\vec{\sigma} \cdot \vec{p}_3}{2m_q} G_3(\vec{p}_3) \end{pmatrix} \chi_{s_{qz}}, \quad (43)$$

$$\psi_{\bar{q}}(\vec{p}_4, s_{\bar{q}z}) = \begin{pmatrix} \frac{\vec{\sigma} \cdot \vec{p}_4}{2m_{\bar{q}}} G_4(\vec{p}_4) \\ G_4(\vec{p}_4) \end{pmatrix} \chi_{s_{\bar{q}z}}, \quad (44)$$

$$\psi_{q'}(\vec{p}_1, s_{q'z}) = \begin{pmatrix} G_1(\vec{p}_1) \\ \frac{\vec{\sigma} \cdot \vec{p}_1}{2m_{q'}} G_1(\vec{p}_1) \end{pmatrix} \chi_{s_{q'z}}, \quad (45)$$

$$\psi_{q'}(\vec{p}_1', s_{q'z}) = \begin{pmatrix} G'_1(\vec{p}_1') \\ \frac{\vec{\sigma} \cdot \vec{p}_1'}{2m_{q'}} G'_1(\vec{p}_1') \end{pmatrix} \chi_{s'_{q'z}}, \quad (46)$$

$$\psi_{\bar{q}'}(\vec{p}_1, s_{\bar{q}'z}) = \begin{pmatrix} \frac{\vec{\sigma} \cdot \vec{p}_1}{2m_{\bar{q}'}} G_1(\vec{p}_1) \\ G_1(\vec{p}_1) \end{pmatrix} \chi_{s_{\bar{q}'z}}, \quad (47)$$

$$\psi_{\bar{q}'}(\vec{p}_1', s'_{\bar{q}'z}) = \begin{pmatrix} \frac{\vec{\sigma} \cdot \vec{p}_1'}{2m_{\bar{q}'}} G'_1(\vec{p}_1') \\ G'_1(\vec{p}_1') \end{pmatrix} \chi_{s'_{\bar{q}'z}}, \quad (48)$$

where $\vec{\sigma}$ are the Pauli matrices; $\chi_{s_{qz}}$, $\chi_{s_{\bar{q}z}}$, $\chi_{s_{q'z}}$, $\chi_{s'_{q'z}}$, $\chi_{s_{\bar{q}'z}}$, and $\chi_{s'_{\bar{q}'z}}$ are the spin wave functions with the magnetic projection quantum numbers, s_{qz} , $s_{\bar{q}z}$, $s_{q'z}$, $s'_{q'z}$, $s_{\bar{q}'z}$, and $s'_{\bar{q}'z}$, of the quark or antiquark spin, respectively. The quark and the antiquark created from the gluon have the same mass, i.e., $m_q = m_{\bar{q}}$.

Keeping terms to order of the inverse of the quark mass, we get

$$\mathcal{M}_{cq'q\bar{q}} = \frac{g_s^2}{k^2} \chi_{s'_{q'z}}^+ \chi_{s_{qz}}^+ T^e T^e G'_1(\vec{p}_1') G_3(\vec{p}_3)$$

$$\left[\frac{\vec{\sigma}(34) \cdot \vec{k}}{2m_q} - \frac{\vec{\sigma}(1) \cdot \vec{\sigma}(34) \vec{\sigma}(1) \cdot \vec{p}_1 + \vec{\sigma}(1) \cdot \vec{p}'_1 \vec{\sigma}(1) \cdot \vec{\sigma}(34)}{2m_{q'}} \right] \\ G_1(\vec{p}_1) G_4(\vec{p}_4) \chi_{s_{\bar{q}'z}} \chi_{s_{\bar{q}z}}, \quad (49)$$

$$\begin{aligned} \mathcal{M}_{c\bar{q}'q\bar{q}} = & -\frac{g_s^2}{k^2} \chi_{s_{\bar{q}'z}}^+ \chi_{s_{qz}}^+ T^e T^e G_1(\vec{p}_1) G_3(\vec{p}_3) \\ & \left[\frac{\vec{\sigma}(34) \cdot \vec{k}}{2m_q} - \frac{\vec{\sigma}(1) \cdot \vec{p}_1 \vec{\sigma}(1) \cdot \vec{\sigma}(34) + \vec{\sigma}(1) \cdot \vec{\sigma}(34) \vec{\sigma}(1) \cdot \vec{p}'_1}{2m_{\bar{q}'}} \right] \\ & G'_1(\vec{p}'_1) G_4(\vec{p}_4) \chi_{s'_{\bar{q}'z}} \chi_{s_{\bar{q}z}}. \end{aligned} \quad (50)$$

Using $T^e T^e = \frac{\vec{\lambda}(1)}{2} \cdot \frac{\vec{\lambda}(34)}{2}$ with $\vec{\lambda}$ being the Gell-Mann matrices, we obtain the transition potential for $q'(p_1) \rightarrow q'(p'_1) + q(p_3) + \bar{q}(-p_4)$,

$$V_{cq'q\bar{q}}(\vec{k}) = \frac{\vec{\lambda}(1)}{2} \cdot \frac{\vec{\lambda}(34)}{2} \frac{g_s^2}{k^2} \left(\frac{\vec{\sigma}(34) \cdot \vec{k}}{2m_q} - \frac{\vec{\sigma}(1) \cdot \vec{p}_1 \vec{\sigma}(1) \cdot \vec{\sigma}(34) + \vec{\sigma}(1) \cdot \vec{\sigma}(34) \vec{\sigma}(1) \cdot \vec{p}'_1}{2m_{\bar{q}'}} \right), \quad (51)$$

and the transition potential for $\bar{q}'(-p_1) \rightarrow \bar{q}'(-p'_1) + q(p_3) + \bar{q}(-p_4)$,

$$V_{c\bar{q}'q\bar{q}}(\vec{k}) = -\frac{\vec{\lambda}(1)}{2} \cdot \frac{\vec{\lambda}(34)}{2} \frac{g_s^2}{k^2} \left(\frac{\vec{\sigma}(34) \cdot \vec{k}}{2m_q} - \frac{\vec{\sigma}(1) \cdot \vec{p}_1 \vec{\sigma}(1) \cdot \vec{\sigma}(34) + \vec{\sigma}(1) \cdot \vec{\sigma}(34) \vec{\sigma}(1) \cdot \vec{p}'_1}{2m_{\bar{q}'}} \right). \quad (52)$$

In Eqs. (51) and (52), $\vec{\lambda}(34)$ ($\vec{\sigma}(34)$) mean that they have matrix elements between the color (spin) wave functions of the final quark and the final antiquark. In Eq. (51), $\vec{\lambda}(1)$ ($\vec{\sigma}(1)$) mean that they have matrix elements between the color (spin) wave functions of the final quark and the initial quark. In Eq. (52), $\vec{\lambda}(1)$ ($\vec{\sigma}(1)$) mean that they have matrix elements between the color (spin) wave functions of the initial antiquark and the final antiquark. Applying Eqs. (51) and (52) to the eight Feynman diagrams, we have

$$V_{D_1} \equiv V_{cq_1q_3\bar{q}_4}, V_{D_2} \equiv V_{c\bar{q}_1q_3\bar{q}_4}, V_{D_3} \equiv V_{cq_2q_3\bar{q}_4}, V_{D_4} \equiv V_{c\bar{q}_2q_3\bar{q}_4}, V_{D_5} \equiv V_{cq_1q_3\bar{q}_4}, V_{D_6} \equiv V_{c\bar{q}_1q_3\bar{q}_4}, \\ V_{D_7} \equiv V_{cq_2q_3\bar{q}_4}, \text{ and } V_{D_8} \equiv V_{c\bar{q}_2q_3\bar{q}_4}.$$

IV. MATRIX ELEMENTS

The transition amplitudes include color, spin, and flavor matrix elements. Denote the spin of meson A (B , C_1 , C_2 , C_3) by S_A (S_B , S_{C_1} , S_{C_2} , S_{C_3}) and its magnetic projection quantum number by S_{Az} (S_{Bz} , S_{C_1z} , S_{C_2z} , S_{C_3z}). Let $\phi_{A\text{rel}}$ ($\phi_{B\text{rel}}$, $\phi_{C_1\text{rel}}$, $\phi_{C_2\text{rel}}$, $\phi_{C_3\text{rel}}$),

$\phi_{A\text{color}}$ ($\phi_{B\text{color}}$, $\phi_{C_1\text{color}}$, $\phi_{C_2\text{color}}$, $\phi_{C_3\text{color}}$), $\phi_{A\text{flavor}}$ ($\phi_{B\text{flavor}}$, $\phi_{C_1\text{flavor}}$, $\phi_{C_2\text{flavor}}$, $\phi_{C_3\text{flavor}}$), and $\chi_{S_A S_{Az}}$ ($\chi_{S_B S_{Bz}}$, $\chi_{S_{C_1} S_{C_1z}}$, $\chi_{S_{C_2} S_{C_2z}}$, $\chi_{S_{C_3} S_{C_3z}}$) be the quark-antiquark relative-motion wave function, the color wave function, the flavor wave function, and the spin wave function of meson A (B , C_1 , C_2 , C_3), respectively. The wave function of mesons A and B is

$$\psi_{AB} = \phi_{A\text{rel}} \phi_{B\text{rel}} \phi_{A\text{color}} \phi_{B\text{color}} \chi_{S_A S_{Az}} \chi_{S_B S_{Bz}} \varphi_{AB\text{flavor}}, \quad (53)$$

and the wave function of mesons C_1 , C_2 , and C_3 is

$$\psi_{C_1 C_2 C_3} = \phi_{C_1\text{rel}} \phi_{C_2\text{rel}} \phi_{C_3\text{rel}} \phi_{C_1\text{color}} \phi_{C_2\text{color}} \phi_{C_3\text{color}} \chi_{S_{C_1} S_{C_1z}} \chi_{S_{C_2} S_{C_2z}} \chi_{S_{C_3} S_{C_3z}} \varphi_{C_1 C_2 C_3\text{flavor}}, \quad (54)$$

where $\psi_{AB} = \psi_{q_1 \bar{q}_1} \psi_{q_2 \bar{q}_2}$ and $\psi_{C_1 C_2 C_3} = \psi_{q_1 \bar{q}_4} \psi_{q_2 \bar{q}_1} \psi_{q_3 \bar{q}_2} = \psi_{q_1 \bar{q}_2} \psi_{q_2 \bar{q}_4} \psi_{q_3 \bar{q}_1}$. The flavor wave function $\varphi_{AB\text{flavor}}$ of mesons A and B possesses the same isospin I as the flavor wave function $\varphi_{C_1 C_2 C_3\text{flavor}}$ of mesons C_1 , C_2 , and C_3 .

The color wave function of each meson is the color singlet. The color wave function of mesons A and B is $\phi_{A\text{color}} \phi_{B\text{color}}$, and the color wave function of mesons C_1 , C_2 , and C_3 is $\phi_{C_1\text{color}} \phi_{C_2\text{color}} \phi_{C_3\text{color}}$. The color matrix element is

$$\phi_{C_1\text{color}}^+ \phi_{C_2\text{color}}^+ \phi_{C_3\text{color}}^+ \frac{\vec{\lambda}}{2} \cdot \frac{\vec{\lambda}(34)}{2} \phi_{A\text{color}} \phi_{B\text{color}},$$

where $\vec{\lambda}$ are the Gell-Mann matrices for the color generators of quark q_1 in diagram D_1 , antiquark \bar{q}_1 in diagram D_2 , quark q_2 in diagram D_3 , antiquark \bar{q}_2 in diagram D_4 , quark q_1 in diagram D_5 , antiquark \bar{q}_1 in diagram D_6 , quark q_2 in diagram D_7 , or antiquark \bar{q}_2 in diagram D_8 . The color matrix element is $\frac{4}{9\sqrt{3}}$, $-\frac{4}{9\sqrt{3}}$, $\frac{4}{9\sqrt{3}}$, $-\frac{4}{9\sqrt{3}}$, $\frac{4}{9\sqrt{3}}$, $-\frac{4}{9\sqrt{3}}$, $\frac{4}{9\sqrt{3}}$, and $-\frac{4}{9\sqrt{3}}$ for diagrams D_1 , D_2 , D_3 , D_4 , D_5 , D_6 , D_7 , and D_8 , respectively.

The flavor wave functions, $\phi_{A\text{flavor}}$ and $\phi_{B\text{flavor}}$, are coupled to the flavor wave function $\varphi_{AB\text{flavor}}$. The flavor wave function of meson C_1 and the one of meson C_2 are coupled to the wave function $\varphi_{C_1 C_2\text{flavor}}$ of mesons C_1 and C_2 with the total isospin $I_{C_1 C_2}^f$. Furthermore, $\varphi_{C_1 C_2\text{flavor}}$ and $\phi_{C_3\text{flavor}}$ are coupled to $\varphi_{C_1 C_2 C_3\text{flavor}}$ with isospin I . Let $P_{q_1 \rightarrow q_1 + q_3 + \bar{q}_4}$ ($P_{\bar{q}_1 \rightarrow \bar{q}_1 + q_3 + \bar{q}_4}$, $P_{q_2 \rightarrow q_2 + q_3 + \bar{q}_4}$, $P_{\bar{q}_2 \rightarrow \bar{q}_2 + q_3 + \bar{q}_4}$) denote the operator that implements $q_1 \rightarrow q_1 + q_3 + \bar{q}_4$ ($\bar{q}_1 \rightarrow \bar{q}_1 + q_3 + \bar{q}_4$, $q_2 \rightarrow q_2 + q_3 + \bar{q}_4$, $\bar{q}_2 \rightarrow \bar{q}_2 + q_3 + \bar{q}_4$). The flavor matrix elements corresponding to diagrams D_1 , D_2 , D_3 , D_4 , D_5 , D_6 , D_7 , and D_8

are defined as

$$\mathcal{M}_{D_1f} = \varphi_{C_1C_2C_3\text{flavor}}^+ P_{q_1 \rightarrow q_1 + q_3 + \bar{q}_4} \varphi_{AB\text{flavor}}, \quad (55)$$

$$\mathcal{M}_{D_2f} = \varphi_{C_1C_2C_3\text{flavor}}^+ P_{\bar{q}_1 \rightarrow \bar{q}_1 + q_3 + \bar{q}_4} \varphi_{AB\text{flavor}}, \quad (56)$$

$$\mathcal{M}_{D_3f} = \varphi_{C_1C_2C_3\text{flavor}}^+ P_{q_2 \rightarrow q_2 + q_3 + \bar{q}_4} \varphi_{AB\text{flavor}}, \quad (57)$$

$$\mathcal{M}_{D_4f} = \varphi_{C_1C_2C_3\text{flavor}}^+ P_{\bar{q}_2 \rightarrow \bar{q}_2 + q_3 + \bar{q}_4} \varphi_{AB\text{flavor}}, \quad (58)$$

for $A(q_1\bar{q}_1) + B(q_2\bar{q}_2) \rightarrow C_1(q_1\bar{q}_4) + C_2(q_2\bar{q}_1) + C_3(q_3\bar{q}_2)$ and

$$\mathcal{M}_{D_5f} = \varphi_{C_1C_2C_3\text{flavor}}^+ P_{q_1 \rightarrow q_1 + q_3 + \bar{q}_4} \varphi_{AB\text{flavor}}, \quad (59)$$

$$\mathcal{M}_{D_6f} = \varphi_{C_1C_2C_3\text{flavor}}^+ P_{\bar{q}_1 \rightarrow \bar{q}_1 + q_3 + \bar{q}_4} \varphi_{AB\text{flavor}}, \quad (60)$$

$$\mathcal{M}_{D_7f} = \varphi_{C_1C_2C_3\text{flavor}}^+ P_{q_2 \rightarrow q_2 + q_3 + \bar{q}_4} \varphi_{AB\text{flavor}}, \quad (61)$$

$$\mathcal{M}_{D_8f} = \varphi_{C_1C_2C_3\text{flavor}}^+ P_{\bar{q}_2 \rightarrow \bar{q}_2 + q_3 + \bar{q}_4} \varphi_{AB\text{flavor}}, \quad (62)$$

for $A(q_1\bar{q}_1) + B(q_2\bar{q}_2) \rightarrow C_1(q_1\bar{q}_2) + C_2(q_2\bar{q}_4) + C_3(q_3\bar{q}_1)$. From the eight Feynman diagrams we have the relation,

$$\mathcal{M}_{D_1f} = \mathcal{M}_{D_2f} = \mathcal{M}_{D_3f} = \mathcal{M}_{D_4f}, \quad (63)$$

$$\mathcal{M}_{D_5f} = \mathcal{M}_{D_6f} = \mathcal{M}_{D_7f} = \mathcal{M}_{D_8f}. \quad (64)$$

We list in Table 1 the flavor matrix elements for the following 2-to-3 meson-meson reactions:

$$\pi\pi \rightarrow \pi K\bar{K}, \quad \pi K \rightarrow \pi\pi K, \quad \pi K \rightarrow K K\bar{K}, \quad K K \rightarrow \pi K K, \quad K\bar{K} \rightarrow \pi K\bar{K},$$

$$\text{where } K = \begin{pmatrix} K^+ \\ K^0 \end{pmatrix} \text{ and } \bar{K} = \begin{pmatrix} \bar{K}^0 \\ K^- \end{pmatrix}.$$

The initial mesons and the final mesons in the five reactions are pseudoscalar mesons. The spin wave function of each pseudoscalar meson is the spin singlet of the quark and the antiquark. The spin wave function of the two initial mesons or the three final mesons is simply the product of the spin wave function of each meson as seen in Eq. (53) or (54). Spin matrix elements are listed in Table 2. In the table $\vec{\sigma}$ are the Pauli matrices for quark q_1 in diagrams D₁ and D₅, antiquark \bar{q}_1 in diagrams D₂ and D₆, quark q_2 in diagrams D₃ and D₇, or antiquark \bar{q}_2 in diagrams D₄ and D₈.

The mesonic quark-antiquark relative-motion wave functions, $\phi_{A\text{rel}}$, $\phi_{B\text{rel}}$, $\phi_{C_1\text{rel}}$, $\phi_{C_2\text{rel}}$, and $\phi_{C_3\text{rel}}$, are the solutions of the Schrödinger equation with the potential [61] between constituents a and b :

$$V_{ab}(\vec{r}) = -\frac{\vec{\lambda}_a}{2} \cdot \frac{\vec{\lambda}_b}{2} \frac{3}{4} D \left[1.3 - \left(\frac{T}{T_c} \right)^4 \right] \tanh(Ar) + \frac{\vec{\lambda}_a}{2} \cdot \frac{\vec{\lambda}_b}{2} \frac{6\pi}{25} \frac{v(\lambda r)}{r} \exp(-Er) \\ - \frac{\vec{\lambda}_a}{2} \cdot \frac{\vec{\lambda}_b}{2} \frac{16\pi^2}{25} \frac{d^3}{\pi^{3/2}} \exp(-d^2 r^2) \frac{\vec{s}_a \cdot \vec{s}_b}{m_a m_b} + \frac{\vec{\lambda}_a}{2} \cdot \frac{\vec{\lambda}_b}{2} \frac{4\pi}{25} \frac{1}{r} \frac{d^2 v(\lambda r)}{dr^2} \frac{\vec{s}_a \cdot \vec{s}_b}{m_a m_b}, \quad (65)$$

in which $D = 0.7$ GeV, $E = 0.6$ GeV, $\lambda = \sqrt{25/16\pi^2\alpha'}$ with $\alpha' = 1.04$ GeV $^{-2}$, and $A = 1.5[0.75 + 0.25(T/T_c)^{10}]^6$ GeV, where T is the temperature and T_c is the critical temperature which equals 0.175 GeV [62]. The function v is given by Buchmüller and Tye in Ref. [63], and the quantity d is given by

$$d^2 = d_1^2 \left[\frac{1}{2} + \frac{1}{2} \left(\frac{4m_a m_b}{(m_a + m_b)^2} \right)^4 \right] + d_2^2 \left(\frac{2m_a m_b}{m_a + m_b} \right)^2, \quad (66)$$

where $d_1 = 0.15$ GeV and $d_2 = 0.705$. The potential is a function of the distance r between constituents a and b , and contains the spins, \vec{s}_a and \vec{s}_b , and the Gell-Mann matrices $\vec{\lambda}_a$ and $\vec{\lambda}_b$. When the masses of the up quark, the down quark, the strange quark, and the charm quark are 0.32 GeV, 0.32 GeV, 0.5 GeV, and 1.51 GeV, respectively, the meson masses obtained from the Schrödinger equation with the potential at zero temperature reproduce the experimental masses of π , ρ , K , K^* , J/ψ , ψ' , χ_c , D , D^* , D_s , and D_s^* mesons [64]. Moreover, the experimental data of S -wave phase shifts for elastic $\pi\pi$ scattering for $I = 2$ in vacuum [2, 3, 6, 10] are reproduced in the Born approximation.

V. NUMERICAL CROSS SECTIONS AND DISCUSSIONS

We consider the following 2-to-3 meson-meson reactions:



The reaction $\pi \bar{K} \rightarrow \pi \pi \bar{K}$ ($\pi \bar{K} \rightarrow K \bar{K} \bar{K}$, $\bar{K} \bar{K} \rightarrow \pi \bar{K} \bar{K}$) has the same cross section as $\pi K \rightarrow \pi \pi K$ ($\pi K \rightarrow K K \bar{K}$, $K K \rightarrow \pi K K$). Cross sections for meson-meson reactions depend on the flavor matrix elements. Based on the flavor matrix elements, cross sections

for some isospin channels of reactions can be obtained from the other isospin channels. Therefore, we calculate cross sections for the following eight channels:

$$\begin{aligned} I = 2 \ I_{\pi K}^f &= \frac{3}{2} \ \pi\pi \rightarrow \pi K \bar{K}, \quad I = 1 \ I_{\pi K}^f = \frac{3}{2} \ \pi\pi \rightarrow \pi K \bar{K}, \\ I = \frac{3}{2} \ I_{\pi K}^f &= \frac{3}{2} \ \pi K \rightarrow \pi\pi K, \quad I = \frac{3}{2} \ I_{\pi K}^f = \frac{1}{2} \ \pi K \rightarrow \pi\pi K, \\ I = \frac{3}{2} \ I_{KK}^f &= 1 \ \pi K \rightarrow K K \bar{K}, \quad I = 1 \ I_{\pi K}^f = \frac{3}{2} \ K K \rightarrow \pi K K, \\ I = 1 \ I_{\pi K}^f &= \frac{1}{2} \ K K \rightarrow \pi K K, \quad I = 1 \ I_{\pi \bar{K}}^f = \frac{3}{2} \ K \bar{K} \rightarrow \pi K \bar{K}. \end{aligned}$$

According to Eq. (40) we calculate the unpolarized cross section at the six temperatures $T/T_c = 0, 0.65, 0.75, 0.85, 0.9$, and 0.95 . We plot the unpolarized cross sections for the eight channels of the reactions in Figs. 4-11. These cross sections are functions of the temperature of hadronic matter and the Mandelstam variable \sqrt{s} .

Every curve in Figs. 4-11 has a peak. Let $\sqrt{s_0}$ be the threshold energy. Denote by d_0 the separation between the peak's location on the \sqrt{s} -axis and the threshold energy. The numerical cross sections shown in Figs. 4-11 are parametrized as

$$\begin{aligned} \sigma^{\text{unpol}}(\sqrt{s}, T) &= a_1 \left(\frac{\sqrt{s} - \sqrt{s_0}}{b_1} \right)^{e_1} \exp \left[e_1 \left(1 - \frac{\sqrt{s} - \sqrt{s_0}}{b_1} \right) \right] \\ &\quad + a_2 \left(\frac{\sqrt{s} - \sqrt{s_0}}{b_2} \right)^{e_2} \exp \left[e_2 \left(1 - \frac{\sqrt{s} - \sqrt{s_0}}{b_2} \right) \right]. \end{aligned} \quad (67)$$

The values of the parameters a_1, b_1, e_1, a_2, b_2 , and e_2 are listed in Tables 3 and 4, where $\sqrt{s_z}$ is the square root of the Mandelstam variable at which the cross section is $1/100$ of the peak cross section.

Since the sum of the masses of the final mesons is larger than the sum of the masses of the initial mesons, the reactions are endothermic. When \sqrt{s} increases from the threshold energy, which is the sum of the masses of the final mesons, the cross section of every reaction shown in Figs. 4-11 increases from zero to a maximum and then decreases. The change of the peak cross section with temperature is obvious, and the peak cross section at $T/T_c = 0.95$ is smallest among the peak cross sections at the six temperatures.

As the temperature increases, values of the central spin-independent potential [the first term and the second term of the right-hand side in Eq. (65)] at large distances become smaller and smaller (confinement becomes weaker and weaker), and the Schrödinger

equation produces increasing meson radii. The weakening confinement with increasing temperature makes combining final quarks and antiquarks into mesons more difficult, and thus reduces the cross sections. In contrast to decreasing peak cross sections caused by weakening confinement, increasing peak cross sections are caused by increasing radii of the initial mesons. When the decrease is faster than the increase, the peak cross section goes down as the temperature changes from a value (for example, $0.65T_c$ in Fig. 8 that show cross sections for $\pi K \rightarrow K K \bar{K}$ for $I = 3/2$ and $I_{KK}^f = 1$) to $0.95T_c$.

With increasing temperature, the meson radii increase. This corresponds to increasing wave functions at small quark-antiquark relative momentum. The relative momentum depends linearly on the three-dimensional momentum \vec{P} of an initial meson in the center-of-mass frame of the two initial mesons,

$$\vec{P}^2 = \frac{1}{4}[s - (m_A + m_B)^2][1 - \frac{(m_A - m_B)^2}{s}]. \quad (68)$$

The small relative momentum may be given by small values of $|\vec{P}|$ and, furthermore, of \sqrt{s} . A consequence is that d_0 listed in Tables 3 and 4 decreases or stays unchanged with increasing temperature. The peak cross section occurs at $\sqrt{s} = m_{C_1} + m_{C_2} + m_{C_3} + d_0$. With increasing temperature, the decrease of the pion and kaon masses [52] in addition to d_0 lead to the decrease of $\sqrt{s} = m_{C_1} + m_{C_2} + m_{C_3} + d_0$.

Cross sections for $\pi K \rightarrow \pi\pi K$ for $I = 3/2$ were measured in Ref. [27], but systematic and statistical uncertainties were not given. The experimental cross section is 0.04 mb at $\sqrt{s} = 0.95$ GeV and 0.16 mb at $\sqrt{s} = 1.15$ GeV. The two data are individually near the values 0.014 mb and 0.2 mb of the present work at zero temperature.

The 2-to-3 meson-meson scattering is caused by a gluon created from a quark or an antiquark and the gluon creates a quark-antiquark pair. If the quark-antiquark pair is $u\bar{u}$ or $d\bar{d}$, we have the reaction $\pi K \rightarrow \pi\pi K$. If the quark-antiquark pair is $s\bar{s}$, we have the reaction $\pi K \rightarrow K K \bar{K}$. Since the up-quark and down-quark masses are smaller than the strange-quark mass, it is more likely to create a $u\bar{u}$ or $d\bar{d}$ pair than a $s\bar{s}$ pair. Therefore, the peak cross sections of $\pi K \rightarrow \pi\pi K$ for $I = 3/2$ at a given temperature in Figs. 6 and 7 are larger than the one of $\pi K \rightarrow K K \bar{K}$ for $I = 3/2$ and $I_{KK}^f = 1$ in Fig. 8.

Some 2-to-3 meson-meson reactions in the present work and some 2-to-2 meson-meson reactions in Ref. [53] have the same initial mesons. We can thus compare the cross sections obtained in the present work and those provided in Ref. [53]. At a given temperature the peak cross section of $\pi\pi \rightarrow \pi K \bar{K}$ for $I = 1$ and $I_{\pi K}^f = 3/2$ in Fig. 5 is smaller than the one of $\pi\pi \rightarrow K \bar{K}^*$ for $I = 1$ in Ref. [53]. Cross sections for $\pi K \rightarrow \pi\pi K$ for $I = 3/2$ are shown in Figs. 6 and 7. According to the flavor matrix elements in Table 1, the cross section for $\pi K \rightarrow \pi\pi K$ for $I = 1/2$ and $I_{\pi K}^f = 3/2$ is 1.6 times the one for $\pi K \rightarrow \pi\pi K$ for $I = 3/2$ and $I_{\pi K}^f = 3/2$, and the cross section for $\pi K \rightarrow \pi\pi K$ for $I = 1/2$ and $I_{\pi K}^f = 1/2$ is 0.25 times the one for $\pi K \rightarrow \pi\pi K$ for $I = 3/2$ and $I_{\pi K}^f = 1/2$. The peak cross section of $\pi K \rightarrow \pi\pi K$ for $I = 1/2$ and $I_{\pi K}^f = 3/2$ is smaller than the one of $\pi K \rightarrow \pi K^*$ for $I = 1/2$ at $T/T_c = 0, 0.65$, and 0.75 , but larger at $T/T_c = 0.85, 0.9$, and 0.95 . The peak cross section of $\pi K \rightarrow \pi\pi K$ for $I = 1/2$ and $I_{\pi K}^f = 1/2$ is smaller than the one of $\pi K \rightarrow \pi K^*$ for $I = 1/2$. The peak cross section of $K \bar{K} \rightarrow \pi K \bar{K}$ for $I = 1$ and $I_{\pi \bar{K}}^f = 3/2$ in Fig. 11 is smaller than the one of $K \bar{K} \rightarrow K \bar{K}^*$ for $I = 1$ at $T/T_c = 0, 0.65, 0.75$, and 0.95 , but larger at $T/T_c = 0.85$ and 0.9 . Therefore, 2-to-3 meson-meson scattering may be as important as inelastic 2-to-2 meson-meson scattering.

The τ decay has been used to study asymptotic freedom of QCD [65, 66]. The τ lepton decays into ν_τ and W which splits into a quark and an antiquark. If the quark or the antiquark emits a virtual gluon which subsequently splits into a quark-antiquark pair, decay modes like $\tau^- \rightarrow \pi^- \bar{K}^0 \nu_\tau$ and $\tau^- \rightarrow K^- K^0 \nu_\tau$ are observed. If the quark and/or the antiquark creates two virtual gluons of which each subsequently splits into a quark-antiquark pair, decay modes like $\tau^- \rightarrow \pi^- \bar{K}^0 \pi^0 \nu_\tau$ and $\tau^- \rightarrow K^- K^0 \pi^0 \nu_\tau$ are observed. That the virtual gluon splits into a quark-antiquark pair also takes place in 2-to-3 meson-meson scattering in the present work, and perturbative QCD is applied to the process.

In perturbative QCD physical observables are usually given by a power series in α_s , which is $g_s^2/4\pi$. If the coupling constant α_s is smaller than 1, the perturbative expansion converges. In the present work the coupling constant is 0.75 from Ref. [63], and is used in the Feynman diagrams shown in Fig. 3.

When we add the gluon propagator, the gluon loop, the quark loop, and the ghost loop to the eight diagrams in Figs. 1 and 2, this generates 312 Feynman diagrams at order α_s^2 . The 312 diagrams and the 8 diagrams in Figs. 1 and 2 do not contain quark-antiquark annihilation. From the annihilation of an initial quark and an initial antiquark as well as the creation of a quark-antiquark pair, we get 14 Feynman diagrams at order α_s^2 . In total, we have 326 diagrams. The calculation of such a large number of diagrams is formidable.

The transition potentials given in Eqs. (51) and (52) consist of terms with the inverse of the quark mass. In obtaining the transition potentials the terms with the inverse of the quark mass cubed are neglected, because they are suppressed by the inverse of the quark mass squared in comparison to the terms in Eqs. (51) and (52).

Nonperturbative effects exist in 2-to-3 meson-meson scattering, and are encoded in the mesonic quark-antiquark wave functions as done in Refs. [67, 68]. The quark-antiquark pair from the virtual gluon combines with spectator quarks and antiquarks from the initial mesons to form three final mesons. The combination involves multi-gluon exchange between the quark and the antiquark, and confinement sets in. While the final mesons are formed, the wave functions are determined.

If two or more mesons are produced in a reaction or a decay, they interact with each other before being detected. The role of final state interactions has been studied in chiral perturbation theory. While two mesons are produced in a photon-photon reaction, final state interactions come from meson loops and meson resonances between the two photons and the final mesons [69, 70]. In reproducing experimental data of $\gamma\gamma$ cross sections, final state interactions are essential. However, in the reaction $\pi N \rightarrow \pi\pi N$ final state interactions cause a correction less than 20 % when the total center-of-mass energy of initial πN is smaller than 2 GeV [71]. In the hadronic decays $\eta \rightarrow 3\pi$, $\eta' \rightarrow 3\pi$, and $\eta' \rightarrow \eta\pi\pi$, final state interactions due to loop corrections and resonances lead to excellent agreement of theoretical decay widths with experimental data, $\pi\pi$ rescattering is shown to be important, but S -wave $\pi\eta$ rescattering effects are small [72, 73]. For decay modes like $D \rightarrow \pi\pi\pi$, $D \rightarrow \bar{K}\pi\pi$, $D \rightarrow K\bar{K}\bar{K}$, $J/\psi \rightarrow \pi\pi\pi$, $J/\psi \rightarrow \phi\pi\pi$, $J/\psi \rightarrow \phi K\bar{K}$, $\bar{B}^0 \rightarrow \pi\pi\pi$, $\bar{B}^0 \rightarrow J/\psi\pi\pi$, $\bar{B}^0 \rightarrow J/\psi\pi\eta$, and $\bar{B}^0 \rightarrow J/\psi K\bar{K}$, the decay amplitude is assumed to be

linearly dependent on amplitudes of rescattering diagrams of two final mesons since the weak interaction is involved [74–82]. Experimental data on these decays may be accounted for.

In the meson-meson collisions that produce three mesons, final state interactions due to resonances and loop corrections exist. For instance, the K^* resonance contributes to $\pi\pi \rightarrow \pi K \bar{K}$ through $\pi\pi \rightarrow K^* \bar{K}$ and $K^* \rightarrow \pi K$; $\pi K \rightarrow \pi\pi K$ may happen through $\pi K \rightarrow \pi\rho K$ and $\rho K \rightarrow \pi K$. If the final state interactions are taken into account, more accurate cross sections are expected, but we do not include the final state interactions in the present work. When the two initial mesons approach each other, they undergo elastic scattering. The initial state interaction may influence the production of the three final mesons, but we do not include the initial state interaction in the present work.

VI. SUMMARY

We have proposed a model to study 2-to-3 meson-meson scattering. A gluon is created from a quark or an antiquark constituent, and subsequently the gluon splits into a quark and an antiquark. This process causes a meson-meson collision to produce three mesons. The transition potential for the process has been derived from the Feynman rules in perturbative QCD. Eight Feynman diagrams at tree level are involved in the 2-to-3 meson-meson scattering. From the S -matrix element we have derived the transition amplitudes corresponding to the eight Feynman diagrams, and from the eight transition amplitudes we have derived the unpolarized cross section. The 2-to-3 reactions among pions and kaons include $\pi\pi \rightarrow \pi K \bar{K}$, $\pi K \rightarrow \pi\pi K$, $\pi K \rightarrow K K \bar{K}$, $K K \rightarrow \pi K K$, and $K \bar{K} \rightarrow \pi K \bar{K}$. We have calculated color, spin, and flavor matrix elements for these reactions. From the cross-section formulas we have obtained numerical unpolarized cross sections for eight isospin channels of the reactions, and the numerical cross section results are parametrized. At zero temperature our cross sections for $\pi K \rightarrow \pi\pi K$ for $I = 3/2$ are near the experimental data. The unpolarized cross sections depend on temperature. The cross section for any isospin channel at a given temperature has a maximum, and the peak cross section of any reaction decreases as the temperature approaches the critical temperature. By comparison

with inelastic 2-to-2 meson-meson scattering, we find that 2-to-3 meson-meson scattering may be as important as inelastic 2-to-2 meson-meson scattering.

ACKNOWLEDGEMENTS

This work was supported by the National Natural Science Foundation of China under Grant No. 11175111.

References

- [1] J. Alitti *et al.*, Nuovo Cimento 35, 1 (1965).
- [2] E. Colton, E. Malamud, P. E. Schlein, A. D. Johnson, V. J. Stenger, and P. G. Wohlmuth, Phys. Rev. D 3, 2028 (1971).
- [3] M. J. Losty, V. Chaloupka, A. Ferrando, L. Montanet, E. Paul, D. Yaffe, A. Ziemiński, J. Alitti, B. Gandois, and J. Louie, Nucl. Phys. B 69, 185 (1974).
- [4] N. M. Cason, P. E. Cannata, A. E. Baumbaugh, J. M. Bishop, N. N. Biswas, L. J. Dauwe, V. P. Kenney, R. C. Ruchti, W. D. Shephard, and J. M. Watson, Phys. Rev. D 28, 1586 (1983).
- [5] Aachen-Berlin-Birmingham-Bonn-Hamburg-London-München Collaboration, Phys. Rev. 138, B897 (1965).
- [6] W. Hoogland *et al.*, Nucl. Phys. B 126, 109 (1977).
- [7] E. A. Alekseeva, A. A. Kartamyshev, V. K. Makar'in, K. N. Mukhin, O. O. Patarakin, M. M. Sulkovskaya, A. F. Sustavov, L. V. Surkova, and L. A. Chernysheva, Sov. Phys. JETP 55, 591 (1982).
- [8] K. Takamatsu, Nucl. Phys. A 675, 312c (2000).
- [9] D. Cohen, T. Ferbel, P. Slattery, and B. Werner, Phys. Rev. D 7, 661 (1973).

- [10] N. B. Durusoy, M. Baubillier, R. George, M. Goldberg, A. M. Touchard, N. Armenise, M. T. Fogli-Muciaccia, and A. Silvestri, Phys. Lett. B 45, 517 (1973).
- [11] S. D. Protopopescu, M. Alston-Garnjost, A. Barbaro-Galtieri, S. M. Flatté, J. H. Friedman, T. A. Lasinski, G. R. Lynch, M. S. Rabin, and F. T. Solmitz, Phys. Rev. D 7, 1279 (1973).
- [12] J. P. Baton, G. Laurens, and J. Reignier, Nucl. Phys. B 3, 349 (1967); Phys. Lett. 33 B, 528 (1970).
- [13] W. D. Walker, J. Carroll, A. Garfinkel, and B. Y. Oh, Phys. Rev. Lett. 18, 630 (1967).
- [14] B. Y. Oh, A. F. Garfinkel, R. Morse, W. D. Walker, J. D. Prentice, E. C. West, and T. S. Yoon, Phys. Rev. D1, 2494 (1970).
- [15] B. Hyams *et al.*, Nucl. Phys. B 64, 134 (1973).
- [16] G. Grayer *et al.*, Nucl. Phys. B 75, 189 (1974).
- [17] P. Estabrooks and A. D. Martin, Nucl. Phys. B 79, 301 (1974).
- [18] V. Srinivasan *et al.*, Phys. Rev. D 12, 681 (1975).
- [19] C. D. Froggatt and J. L. Petersen, Nucl. Phys. B 129, 89 (1977).
- [20] A. A. Bel'kov, S. A. Bunyatov, K. N. Mukhin, O. O. Patarakin, V. M. Sidorov, M. M. Sulkovskaya, A. F. Sustavov, and V. A. Yarba, JETP Lett. 29, 597 (1979).
- [21] R. Kamiński, L. Leśniak, K. Rybicki, Z. Phys. C 74, 79 (1997).
- [22] L. Rosselet *et al.*, Phys. Rev. D 15, 574 (1977).
- [23] S. Pisłak *et al.*, Phys. Rev. D 67, 072004 (2003).
- [24] R. García-Martín, R. Kamiński, J. R. Peláez, J. R. de Elvira, and F. J. Ynduráin, Phys. Rev. D 83, 074004 (2011).

- [25] J. R. Batley *et al.*, Eur. Phys. J. C 54, 411 (2008).
- [26] R. Mercer *et al.*, Nucl. Phys. B 32, 381 (1971).
- [27] B. Jongejans, R. A. van Meurs, A. G. Tenner, H. Voorthuis, P. M. Heinen, W. J. Metzger, H. G. J. M. Tiecke, and R. T. Van de Walle, Nucl. Phys. B 67, 381 (1973).
- [28] D. Linglin *et al.*, Nucl. Phys. B 57, 64 (1973).
- [29] P. Estabrooks, R. K. Carnegie, A. D. Martin, W. M. Dunwoodie, T. A. Lasinski, and D. W. G. S. Leith, Nucl. Phys. B 133, 490 (1978).
- [30] D. Aston *et al.*, Nucl. Phys. B 296, 493 (1988).
- [31] P. del Amo Sanchez *et al.*, Phys. Rev. D 83, 072001 (2011).
- [32] D. Cohen, D. S. Ayres, R. Diebold, S. L. Kramer, A. J. Pawlicki, and A. B. Wicklund, Phys. Rev. D 22, 2595 (1980).
- [33] S. M. Roy, Phys. Lett. B 36, 353 (1971); M. R. Pennington and S. D. Protopopescu, Phys. Rev. D 7, 1429 (1973); B. Ananthanarayan, Phys. Rev. D 58, 036002 (1998); G. Colangelo, J. Gasser, and H. Leutwyler, Nucl. Phys. B 603, 125 (2001); R. Kamiński, L. Leśniak, and B. Loiseau, Phys. Lett. B 551, 241 (2003).
- [34] J. Gasser and H. Leutwyler, Ann. Phys. 158, 142 (1984); J. Gasser and H. Leutwyler, Nucl. Phys. B 250, 465 (1985); J. Gasser and U. G. Meissner, Phys. Lett. B 258, 219 (1991); J. Gasser and U. G. Meissner, Nucl. Phys. B 357, 90 (1991); I. Bijnens, G. Colangelo, G. Ecker, J. Gasser, M. E. Sainio, Nucl. Phys. B 508, 263 (1997).
- [35] T. N. Truong, Phys. Rev. Lett. 61, 2526 (1988); A. Dobado, M. J. Herrero, and T. N. Truong, Phys. Lett. B 235, 134 (1990); S. Willenbrock, Phys. Rev. D 43, 1710 (1991); G.-Y. Qin, W. Z. Deng, Z. G. Xiao, and H. Q. Zheng, Phys. Lett. B 542, 89 (2002).
- [36] T. N. Truong, Phys. Rev. Lett. 67, 2260 (1991); T. Hannah, Phys. Rev. D 55, 5613 (1997); A. Dobado and J. R. Peláez, Phys. Rev. D 56, 3057 (1997); M. Boglione and

M. R. Pennington, Z. Phys. C 75, 113 (1997); J. A. Oller, E. Oset, and J. R. Peláez, Phys. Rev. D 59, 074001 (1999); J. Nieves, M. P. Valderrama, and E. R. Arriola, Phys. Rev. D 65, 036002 (2002); J. Nebreda and J. R. Peláez, Phys. Rev. D 81, 054035 (2010); M. Döring and U.-G. Meißner, JHEP 01, 009 (2012).

- [37] F. Guerrero and J. A. Oller, Nucl. Phys. B 537, 459 (1999); A. G. Nicola and J. Peláez, Phys. Rev. D 65, 054009 (2002).
- [38] B. S. Zou and D. V. Bugg, Phys. Rev. D 50, 591 (1994); L. Li, B. S. Zou, and G.-L. Li, Phys. Rev. D 67, 034025 (2003); F. Q. Wu, B. S. Zou, L. Li, and D. V. Bugg, Nucl. Phys. A 735, 111 (2004).
- [39] A. Dobado and J. R. Peláez, Phys. Lett. B 286, 136 (1992); A. Dobado and J. Morales, Phys. Rev. D 52, 2878 (1995).
- [40] G. Janssen, B. C. Pearce, K. Holinde, and J. Speth, Phys. Rev. D 52, 2690 (1995); B. A. Li, Phys. Rev. D 52, 5165 (1995); B. A. Li, D.-N. Gao, and M.-L. Yan, Phys. Rev. D 58, 094031 (1998); D. Black, A. H. Fariborz, and J. Schechter, Phys. Rev. D 61, 074030 (2000).
- [41] J. A. Oller and E. Oset, Nucl. Phys. A 620, 438 (1997); F.-K. Guo, R.-G. Ping, P.-N. Shen, H.-C. Chiang, and B. S. Zou, Nucl. Phys. A 773, 78 (2006); I. V. Danilkin, L. I. R. Gil, and M. F. M. Lutz, Phys. Lett. B 703, 504 (2011); Z.-H. Guo, L. Liu, U.-G. Meißner, J. A. Oller, and A. Rusetsky, Phys. Rev. D 95, 054004 (2017); I. V. Danilkin and M. Vanderhaeghen, Phys. Lett. B 789, 366 (2019).
- [42] J. S. Borges, J. S. Barbosa, and V. Oguri, Phys. Lett. B 393, 413 (1997); Phys. Lett. B 412, 389 (1997).
- [43] J. V. Steele, H. Yamagishi, and I. Zahed, Nucl. Phys. A 615, 305 (1997).
- [44] J. Nieves and E. R. Arriola, Phys. Lett. B 455, 30 (1999); M. Albaladejo, J. A. Oller, E. Oset, G. Rios, and L. Roca, JHEP 08, 071 (2012).

- [45] J. A. Oller and E. Oset, Phys. Rev. D 60, 074023 (1999); M. Albaladejo, J. A. Oller, and L. Roca, Phys. Rev. D 82, 094019 (2010).
- [46] T. Barnes and E. S. Swanson, Phys. Rev. D 46, 131 (1992); E. S. Swanson, Ann. Phys. (N.Y.) 220, 73 (1992); T. Barnes, E. S. Swanson, and J. Weinstein, Phys. Rev. D 46, 4868 (1992); T. Barnes, N. Black, and E. S. Swanson, Phys. Rev. C 63, 025204 (2001).
- [47] V. Flaminio, W. G. Moorhead, D. R. O. Morrison, N. Rivoire, CERN, Geneva Report No. CERN-HERA-84-01, 1984.
- [48] C. M. Ko, Phys. Rev. C 23, 2760 (1981).
- [49] K. Yang, X.-M. Xu, and H. J. Weber, Phys. Rev. D 96, 114025 (2017).
- [50] D. Lohse, J. W. Durso, K. Holinde, and J. Speth, Nucl. Phys. A 516, 513 (1990).
- [51] G. E. Brown, C. M. Ko, Z. G. Wu, and L. H. Xia, Phys. Rev. C 43, 1881 (1991).
- [52] Y.-Q. Li and X.-M. Xu, Nucl. Phys. A 794, 210 (2007); Z.-Y. Shen and X.-M. Xu, J. Korean Phys. Soc. 66, 754 (2015).
- [53] Z.-Y. Shen, X.-M. Xu, and H. J. Weber, Phys. Rev. D 94, 034030 (2016); T.-T. Wang and X.-M. Xu, Chin. Phys. C 43, 024102 (2019).
- [54] J. R. Peláez and A. Rodas, Eur. Phys. J. C 78, 897 (2018).
- [55] M. Albaladejo and J. A. Oller, Phys. Rev. Lett. 101, 252002 (2008).
- [56] ATLAS Collaboration, Phys. Lett. B 790, 108 (2019).
- [57] CMS Collaboration, JHEP 10, 138 (2018).
- [58] ALICE Collaboration, Phys. Lett. B 788, 166 (2019).
- [59] J. D. Bjorken and S. D. Drell, *Relativistic Quantum Mechanics* (McGraw-Hill, New York, 1964).

- [60] T. Muta, *Foundations of Quantum Chromodynamics* (World Scientific, Singapore, 1987).
- [61] S.-T. Ji, Z.-Y. Shen, and X.-M. Xu, J. Phys. G 42, 095110 (2015).
- [62] F. Karsch, E. Laermann, and A. Peikert, Nucl. Phys. B 605, 579 (2001).
- [63] W. Buchmüller and S.-H. H. Tye, Phys. Rev. D 24, 132 (1981).
- [64] K. Nakamura *et al.* (Particle Data Group), J. Phys. G 37, 075021 (2010).
- [65] P. A. Baikov, K. G. Chetyrkin, and J. H. Kühn, Phys. Rev. Lett. 101, 012002 (2008).
- [66] M. Davier, S. Descotes-Genon, A. Höcker, B. Malaescu, and Z. Zhang, Eur. Phys. J. C 56, 305 (2008).
- [67] P. Kroll, B. Quadder, and W. Schweiger, Nucl. Phys. B 316, 373 (1989).
- [68] A. T. Goritschnig, P. Kroll, and W. Schweiger, Eur. Phys. J. A 42, 43 (2009).
- [69] J. A. Oller and E. Oset, Nucl. Phys. A 629, 739 (1998).
- [70] G. Mennessier, S. Narison, and X.-G. Wang, Phys. Lett. B 696, 40 (2011).
- [71] I. J. R. Aitchison and J. J. Brehm, Phys. Lett. 84 B, 349 (1979).
- [72] B. Borasoy and R. Nifler, Eur. Phys. J. A 26, 383 (2005).
- [73] S. González-Solis and E. Passemar, Eur. Phys. J. C 78, 758 (2018).
- [74] J. A. Oller, Phys. Rev. D 71, 054030 (2005).
- [75] S. X. Nakamura, Phys. Rev. D 93, 014005 (2016).
- [76] R. T. Aoude, P. C. Magalhães, A. C. dos Reis, and M. R. Robilotta, Phys. Rev. D 98, 056021 (2018).
- [77] D. Morgan and M. R. Pennington, Phys. Rev. D 48, 1185 (1993).

- [78] U.-G. Meißner and J. A. Oller, Nucl. Phys. A 679, 671 (2001).
- [79] L. Roca, J. E. Palomar, E. Oset, and H. C. Chiang, Nucl. Phys. A 744, 127 (2004).
- [80] P. Guo, R. Mitchell, and A. P. Szczepaniak, Phys. Rev. D 82, 094002 (2010).
- [81] S. Gardner and U.-G. Meißner, Phys. Rev. D 65, 094004 (2002).
- [82] M. Albaladejo, J. T. Daub, C. Hanhart, B. Kubis, and B. Moussallam, JHEP 04, 010 (2017).

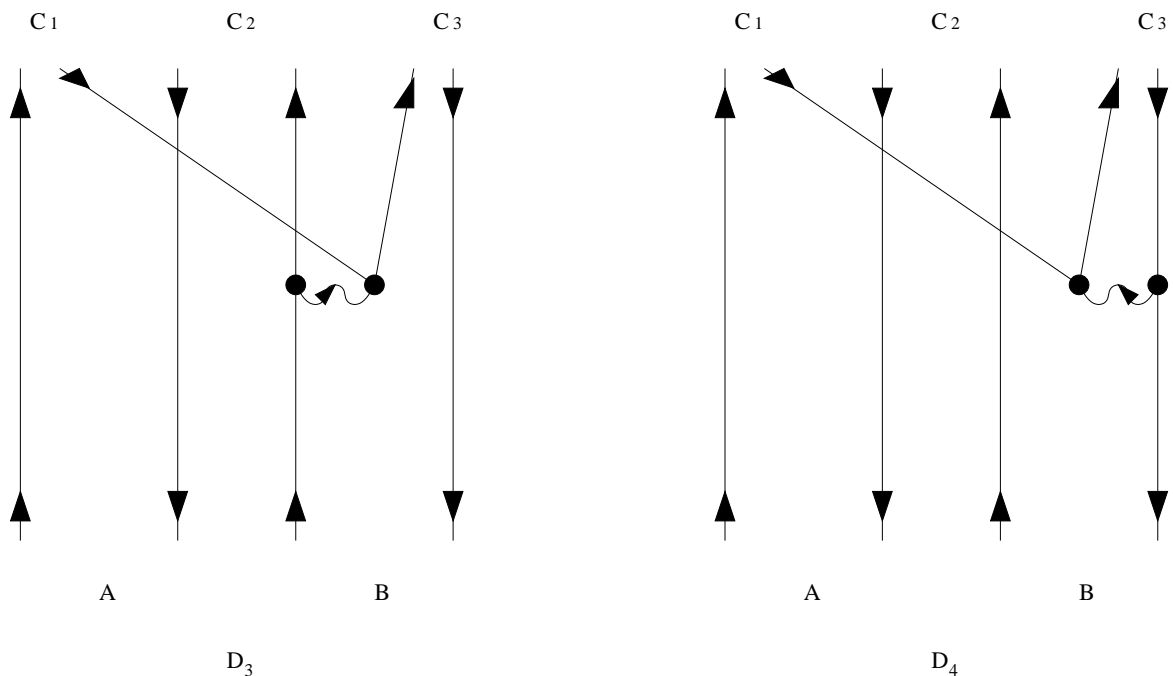
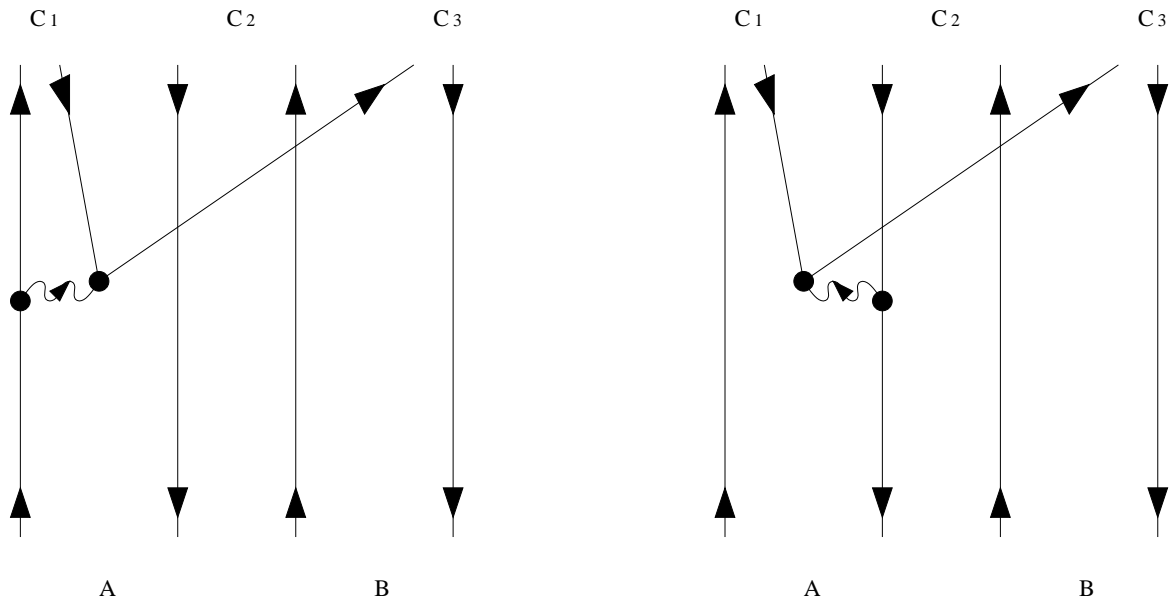


Figure 1: Reaction $A(q_1\bar{q}_1) + B(q_2\bar{q}_2) \rightarrow C_1(q_1\bar{q}_4) + C_2(q_2\bar{q}_1) + C_3(q_3\bar{q}_2)$. Solid lines with up (down) arrows represent quarks (antiquarks). Wavy lines represent gluons.

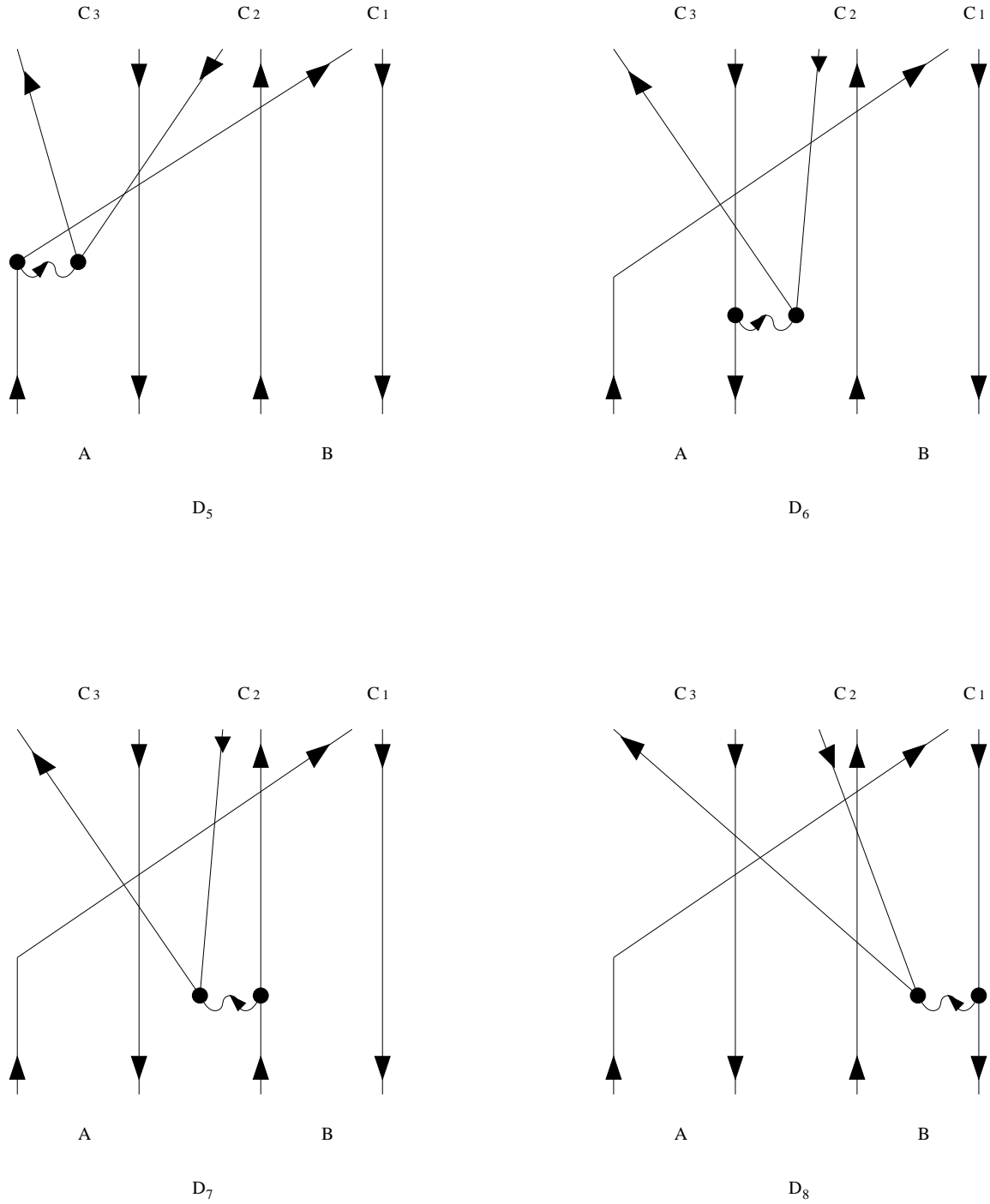


Figure 2: Reaction $A(q_1\bar{q}_1) + B(q_2\bar{q}_2) \rightarrow C_1(q_1\bar{q}_2) + C_2(q_2\bar{q}_4) + C_3(q_3\bar{q}_1)$. Solid lines with up (down) arrows represent quarks (antiquarks). Wavy lines represent gluons.

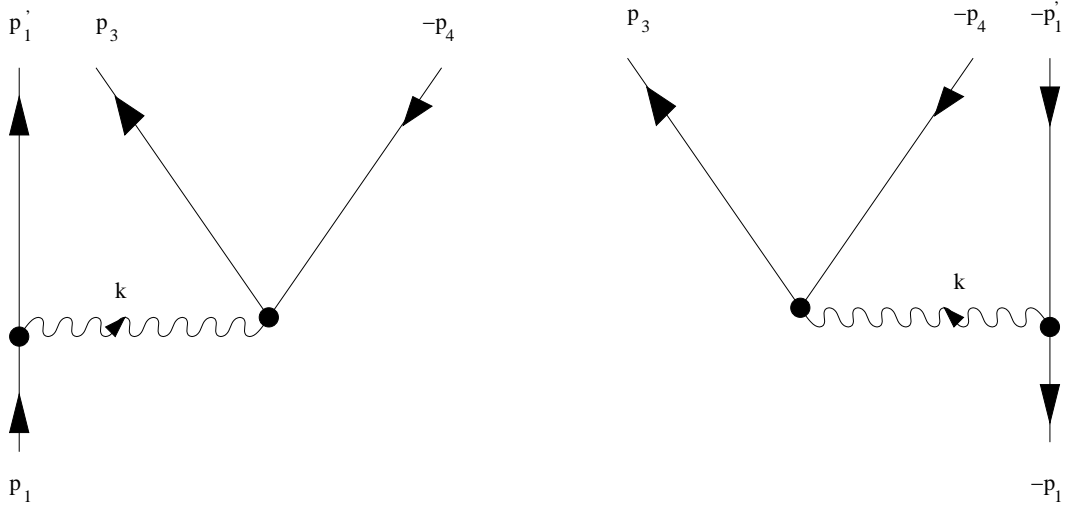


Figure 3: Left diagram with $q'(p_1) \rightarrow q'(p'_1) + q(p_3) + \bar{q}(-p_4)$ and right diagram with $\bar{q}'(-p_1) \rightarrow \bar{q}'(-p'_1) + q(p_3) + \bar{q}(-p_4)$.

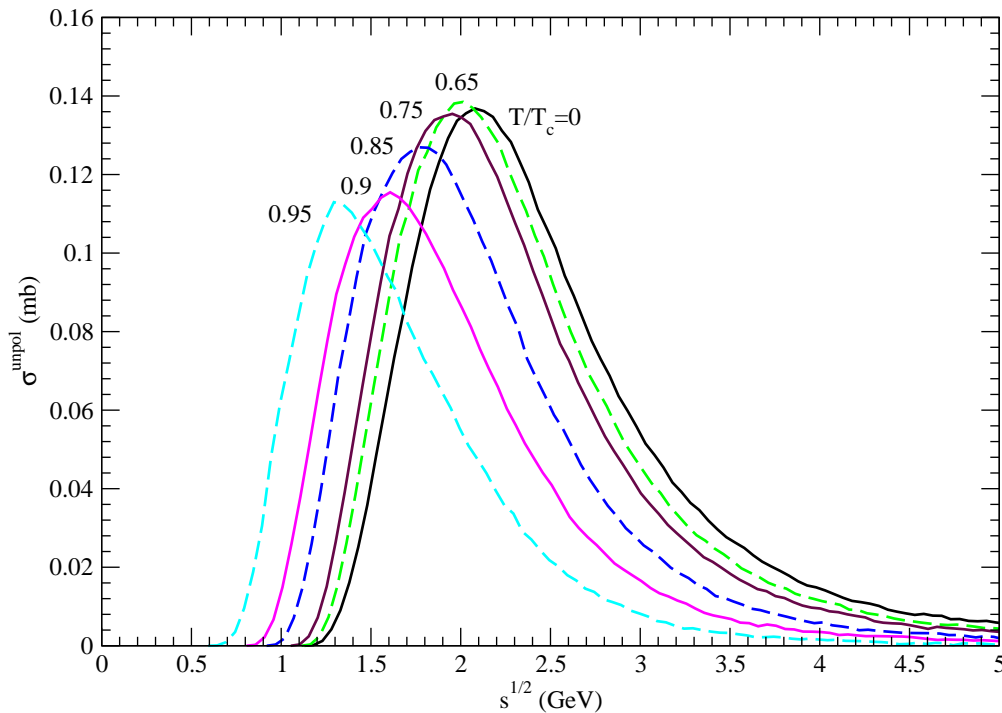


Figure 4: Cross sections for $\pi\pi \rightarrow \pi K \bar{K}$ for $I = 2$ and $I_{\pi K}^f = 3/2$ at various temperatures (in units of the critical temperature).

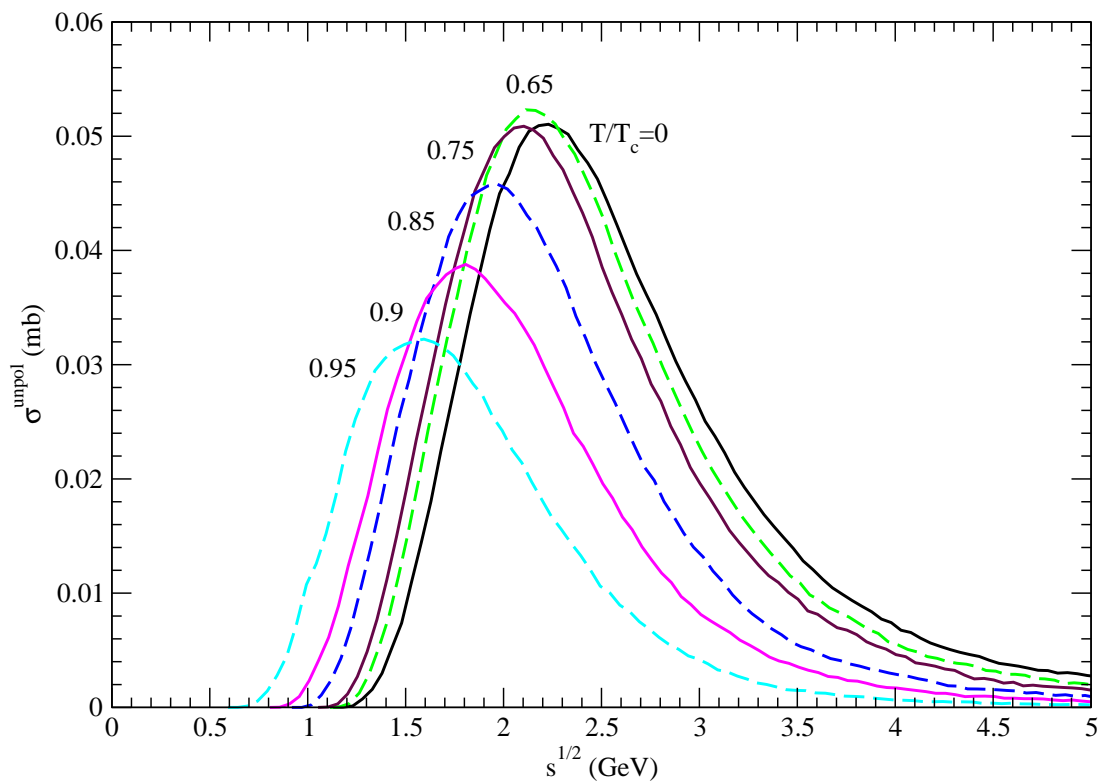


Figure 5: Cross sections for $\pi\pi \rightarrow \pi K \bar{K}$ for $I = 1$ and $I_{\pi K}^f = 3/2$ at various temperatures.

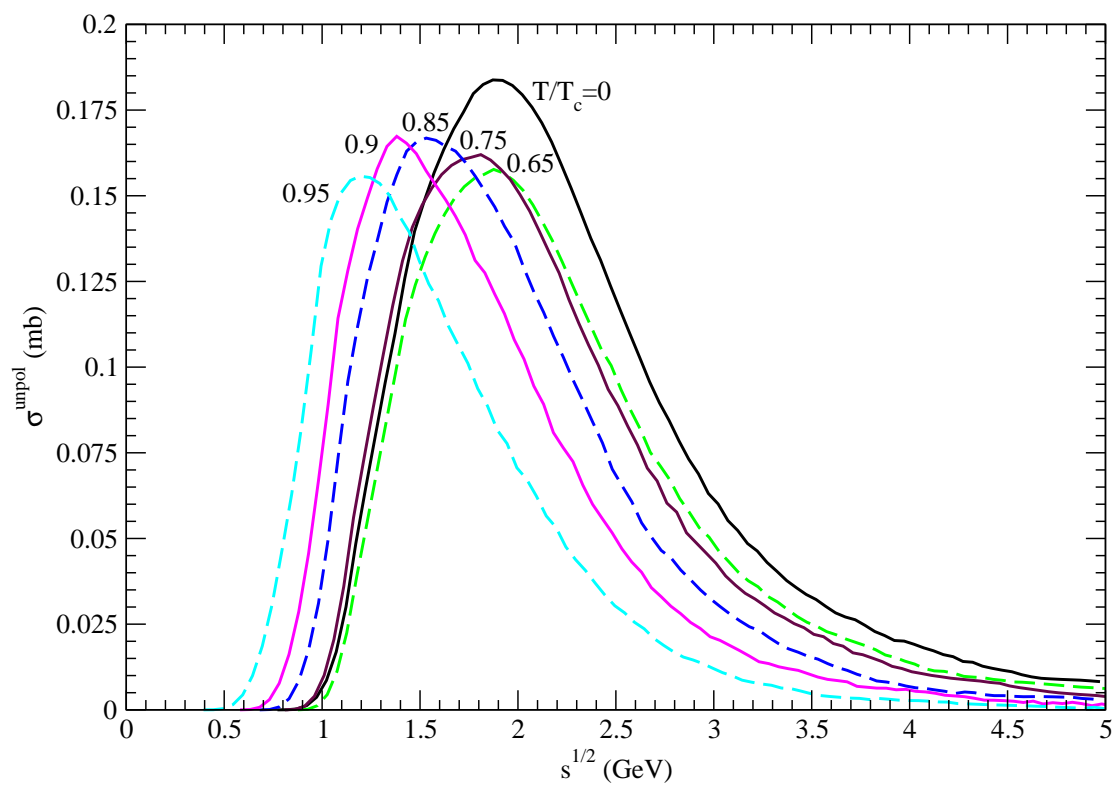


Figure 6: Cross sections for $\pi K \rightarrow \pi\pi K$ for $I = 3/2$ and $I_{\pi K}^f = 3/2$ at various temperatures.

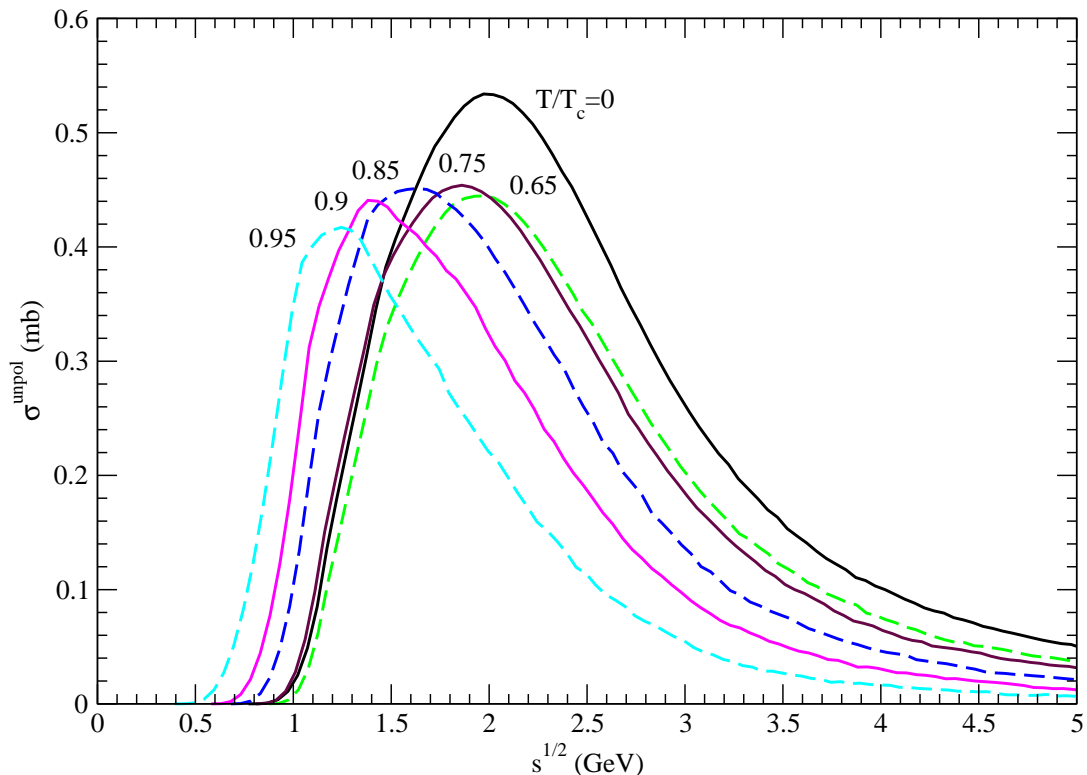


Figure 7: Cross sections for $\pi K \rightarrow \pi\pi K$ for $I = 3/2$ and $I_{\pi K}^f = 1/2$ at various temperatures.

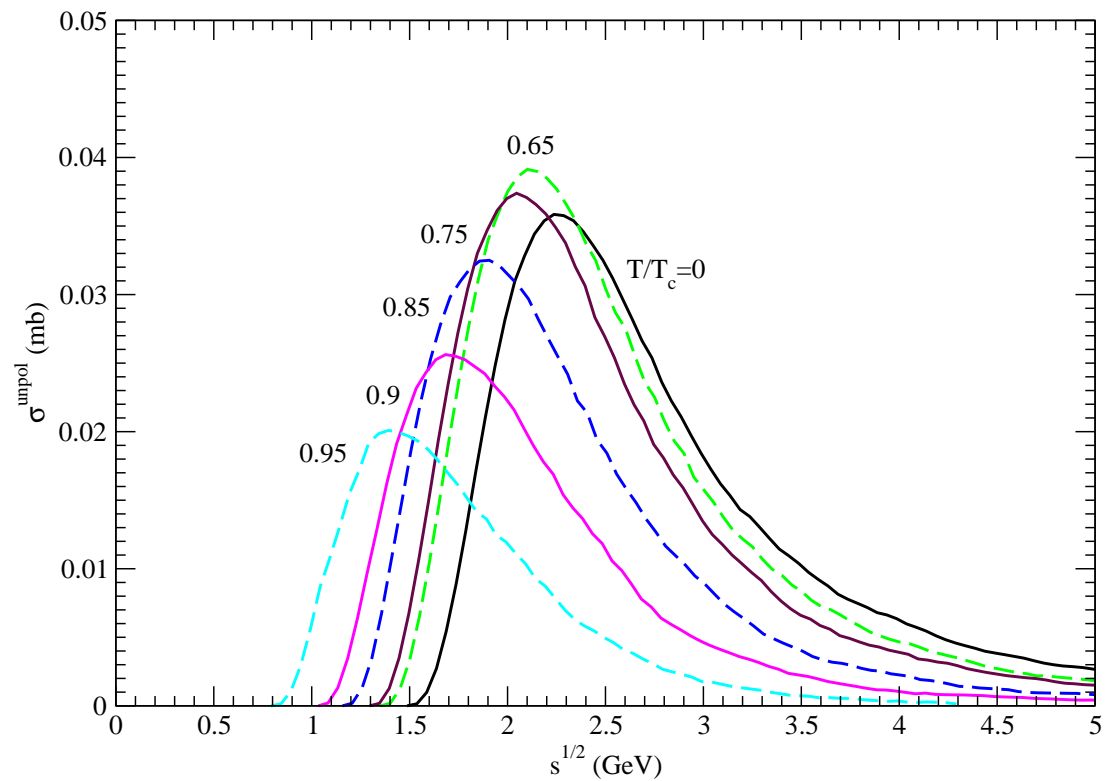


Figure 8: Cross sections for $\pi K \rightarrow K K \bar{K}$ for $I = 3/2$ and $I_{KK}^f = 1$ at various temperatures.

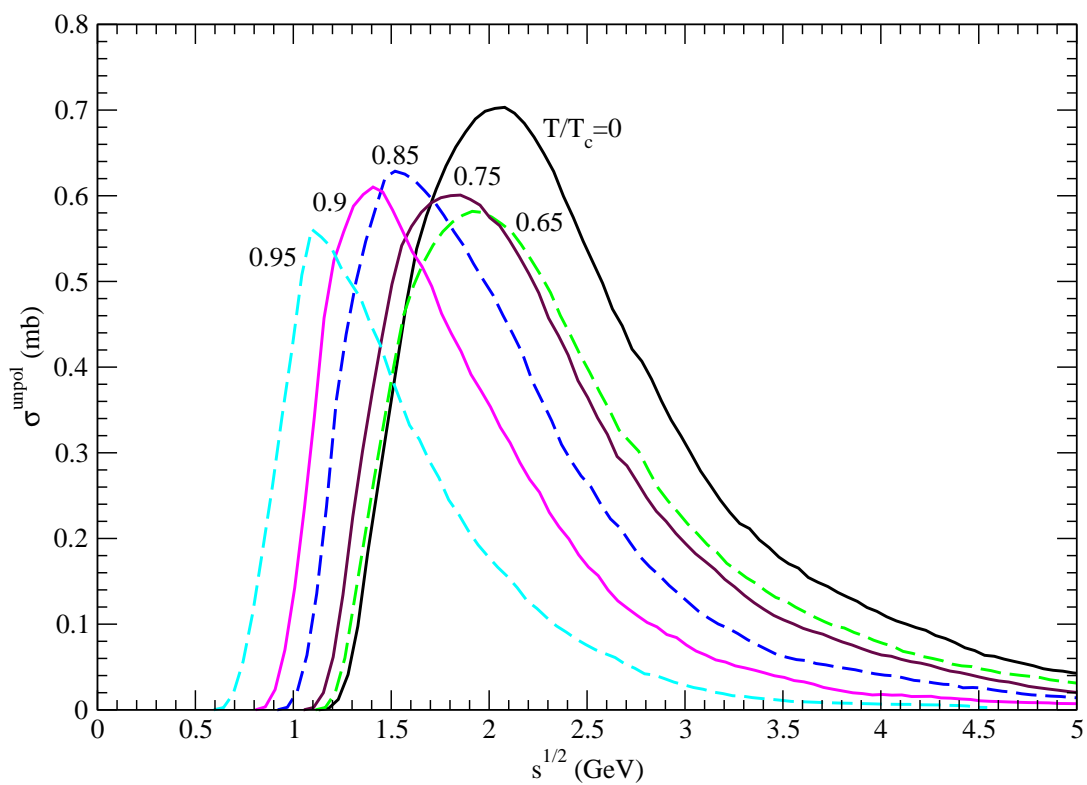


Figure 9: Cross sections for $KK \rightarrow \pi KK$ for $I = 1$ and $I_{\pi K}^f = 3/2$ at various temperatures.

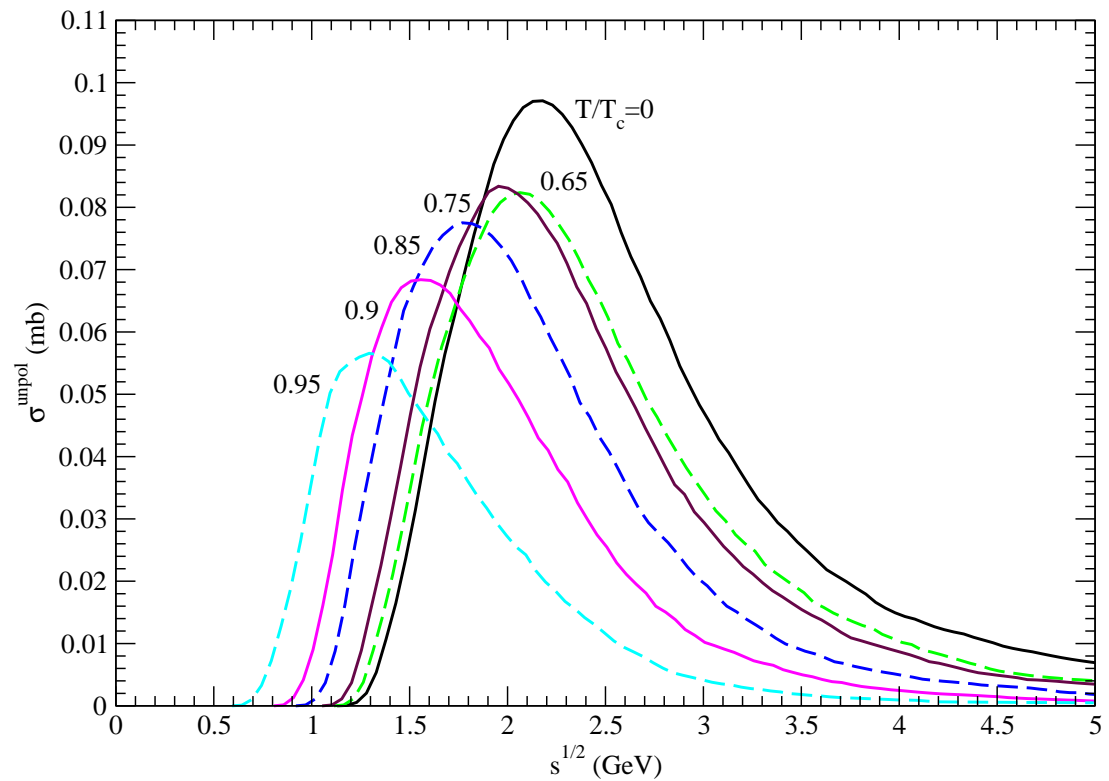


Figure 10: Cross sections for $KK \rightarrow \pi KK$ for $I = 1$ and $I_{\pi K}^f = 1/2$ at various temperatures.

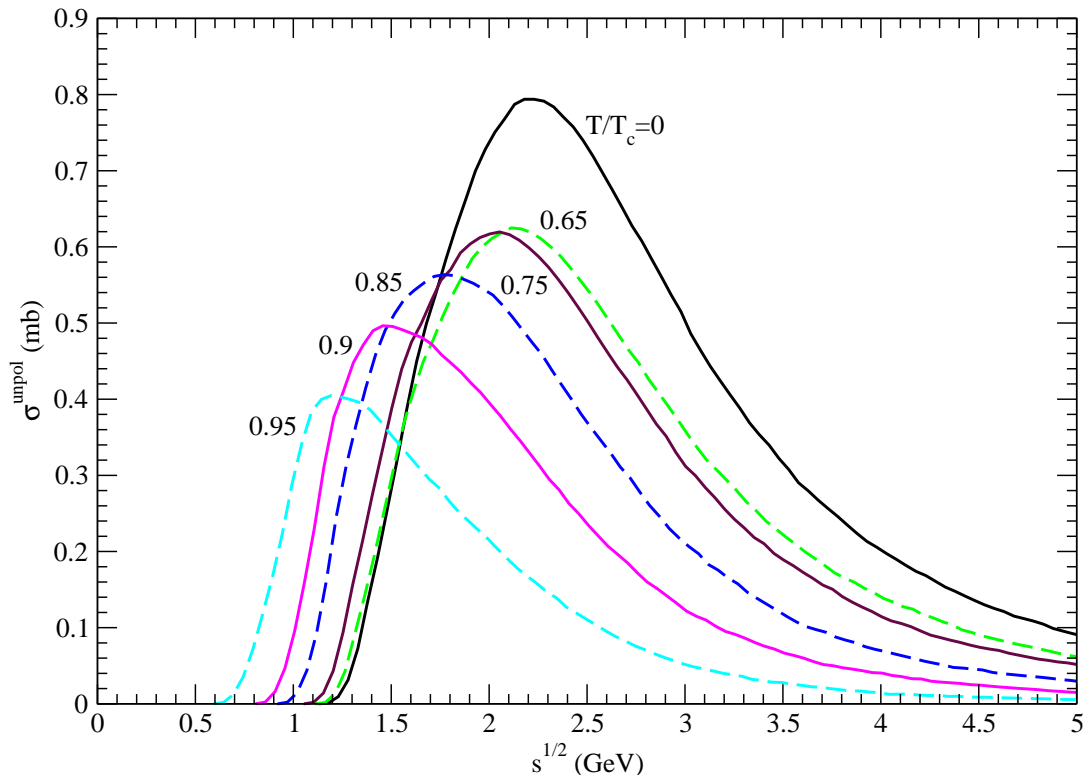


Figure 11: Cross sections for $K\bar{K} \rightarrow \pi K\bar{K}$ for $I = 1$ and $I_{\pi\bar{K}}^f = 3/2$ at various temperatures.

Table 1: Flavor matrix elements in the second column are part of $\mathcal{M}_{D_{1f}}$, $\mathcal{M}_{D_{2f}}$, $\mathcal{M}_{D_{3f}}$, and $\mathcal{M}_{D_{4f}}$, and in the third column of $\mathcal{M}_{D_{5f}}$, $\mathcal{M}_{D_{6f}}$, $\mathcal{M}_{D_{7f}}$, and $\mathcal{M}_{D_{8f}}$.

$I = 2$	$I_{\pi K}^f = \frac{3}{2}$ $\pi\pi \rightarrow \pi K \bar{K}$	1	1
$I = 1$	$I_{\pi K}^f = \frac{3}{2}$ $\pi\pi \rightarrow \pi K \bar{K}$	$\frac{\sqrt{3}}{3}$	$-\frac{\sqrt{3}}{3}$
$I = 1$	$I_{\pi K}^f = \frac{1}{2}$ $\pi\pi \rightarrow \pi K \bar{K}$	$\frac{1}{\sqrt{6}}$	$\frac{1}{\sqrt{6}}$
$I = 0$	$I_{\pi K}^f = \frac{1}{2}$ $\pi\pi \rightarrow \pi K \bar{K}$	$\frac{1}{2}$	$-\frac{1}{2}$
$I = \frac{3}{2}$	$I_{\pi K}^f = \frac{3}{2}$ $\pi K \rightarrow \pi\pi K$	0	$\sqrt{\frac{5}{6}}$
$I = \frac{1}{2}$	$I_{\pi K}^f = \frac{3}{2}$ $\pi K \rightarrow \pi\pi K$	0	$\frac{2}{\sqrt{3}}$
$I = \frac{3}{2}$	$I_{\pi K}^f = \frac{1}{2}$ $\pi K \rightarrow \pi\pi K$	$-\sqrt{\frac{3}{2}}$	$-\frac{1}{\sqrt{6}}$
$I = \frac{1}{2}$	$I_{\pi K}^f = \frac{1}{2}$ $\pi K \rightarrow \pi\pi K$	$-\frac{1}{2}\sqrt{\frac{3}{2}}$	$-\frac{1}{2\sqrt{6}}$
$I = \frac{3}{2}$	$I_{KK}^f = 1$ $\pi K \rightarrow K K \bar{K}$	0	1
$I = \frac{1}{2}$	$I_{KK}^f = 1$ $\pi K \rightarrow K K \bar{K}$	0	$-\frac{1}{2}$
$I = \frac{1}{2}$	$I_{KK}^f = 0$ $\pi K \rightarrow K K \bar{K}$	0	$\frac{\sqrt{3}}{2}$
$I = 1$	$I_{\pi K}^f = \frac{3}{2}$ $K K \rightarrow \pi K K$	$-\frac{2}{\sqrt{3}}$	$-\frac{2}{\sqrt{3}}$
$I = 1$	$I_{\pi K}^f = \frac{1}{2}$ $K K \rightarrow \pi K K$	$-\frac{1}{\sqrt{6}}$	$\frac{1}{\sqrt{6}}$
$I = 0$	$I_{\pi K}^f = \frac{1}{2}$ $K K \rightarrow \pi K K$	$-\frac{3}{\sqrt{6}}$	$-\frac{3}{\sqrt{6}}$
$I = 1$	$I_{\pi \bar{K}}^f = \frac{3}{2}$ $K \bar{K} \rightarrow \pi K \bar{K}$	0	$-\frac{2}{\sqrt{3}}$
$I = 1$	$I_{\pi \bar{K}}^f = \frac{1}{2}$ $K \bar{K} \rightarrow \pi K \bar{K}$	0	$\frac{\sqrt{6}}{3}$
$I = 0$	$I_{\pi \bar{K}}^f = \frac{1}{2}$ $K \bar{K} \rightarrow \pi K \bar{K}$	0	0

Table 2: Spin matrix elements in \mathcal{M}_{D_1} , \mathcal{M}_{D_2} , \mathcal{M}_{D_3} , \mathcal{M}_{D_4} , \mathcal{M}_{D_5} , \mathcal{M}_{D_6} , \mathcal{M}_{D_7} , and \mathcal{M}_{D_8} , which are shown from the second to ninth columns, respectively. The initial spin state is $\phi_{iss} = \chi_{S_A S_{Az}} \chi_{S_B S_{Bz}}$, and the final spin state $\phi_{fss} = \chi_{S_{C_1} S_{C_1z}} \chi_{S_{C_2} S_{C_2z}} \chi_{S_{C_3} S_{C_3z}}$. The z components of the meson spins are $S_{Az} = S_{Bz} = S_{C_1z} = S_{C_2z} = S_{C_3z} = 0$.

$\phi_{fss}^+ \phi_{iss}$	0	0	0	0	0	0	0	0
$\phi_{fss}^+ \sigma_1(34) \phi_{iss}$	0	0	0	0	0	0	0	0
$\phi_{fss}^+ \sigma_2(34) \phi_{iss}$	$-\frac{1}{2\sqrt{2}}i$							
$\phi_{fss}^+ \sigma_3(34) \phi_{iss}$	0	0	0	0	0	0	0	0
$\phi_{fss}^+ \sigma_1 \phi_{iss}$	0	0	0	0	0	0	0	0
$\phi_{fss}^+ \sigma_2 \phi_{iss}$	$-\frac{1}{2\sqrt{2}}i$							
$\phi_{fss}^+ \sigma_3 \phi_{iss}$	0	0	0	0	0	0	0	0
$\phi_{fss}^+ \sigma_1(34) \sigma_1 \phi_{iss}$	0	0	0	0	0	0	0	0
$\phi_{fss}^+ \sigma_1(34) \sigma_2 \phi_{iss}$	0	0	0	0	0	0	0	0
$\phi_{fss}^+ \sigma_1(34) \sigma_3 \phi_{iss}$	$\frac{1}{2\sqrt{2}}$	$-\frac{1}{2\sqrt{2}}$	$\frac{1}{2\sqrt{2}}$	$-\frac{1}{2\sqrt{2}}$	$\frac{1}{2\sqrt{2}}$	$-\frac{1}{2\sqrt{2}}$	$\frac{1}{2\sqrt{2}}$	$-\frac{1}{2\sqrt{2}}$
$\phi_{fss}^+ \sigma_2(34) \sigma_1 \phi_{iss}$	0	0	0	0	0	0	0	0
$\phi_{fss}^+ \sigma_2(34) \sigma_2 \phi_{iss}$	0	0	0	0	0	0	0	0
$\phi_{fss}^+ \sigma_2(34) \sigma_3 \phi_{iss}$	0	0	0	0	0	0	0	0
$\phi_{fss}^+ \sigma_3(34) \sigma_1 \phi_{iss}$	$-\frac{1}{2\sqrt{2}}$	$\frac{1}{2\sqrt{2}}$	$-\frac{1}{2\sqrt{2}}$	$\frac{1}{2\sqrt{2}}$	$-\frac{1}{2\sqrt{2}}$	$\frac{1}{2\sqrt{2}}$	$-\frac{1}{2\sqrt{2}}$	$\frac{1}{2\sqrt{2}}$
$\phi_{fss}^+ \sigma_3(34) \sigma_2 \phi_{iss}$	0	0	0	0	0	0	0	0
$\phi_{fss}^+ \sigma_3(34) \sigma_3 \phi_{iss}$	0	0	0	0	0	0	0	0

Table 3: Values of the parameters. a_1 and a_2 are in units of millibarns; b_1 , b_2 , d_0 , and $\sqrt{s_z}$ are in units of GeV; e_1 and e_2 are dimensionless.

Reactions	T/T_c	a_1	b_1	e_1	a_2	b_2	e_2	d_0	$\sqrt{s_z}$
$I = 2 \ I_{\pi K}^f = \frac{3}{2} \ \pi\pi \rightarrow \pi K \bar{K}$	0	0.1	0.81	3.81	0.05	1.4	5.06	0.95	5.83
	0.65	0.09	0.72	3.24	0.06	1.19	4.12	0.9	5.82
	0.75	0.09	0.71	3.37	0.06	1.18	4.16	0.9	5.6
	0.85	0.08	0.64	3.69	0.07	1.13	4.59	0.85	5.06
	0.9	0.07	0.62	3.57	0.06	1.07	4.31	0.8	5.01
	0.95	0.07	0.6	4.95	0.06	1.05	4.68	0.7	4.26
$I = 1 \ I_{\pi K}^f = \frac{3}{2} \ \pi\pi \rightarrow \pi K \bar{K}$	0	0.03	1.04	4.88	0.02	1.27	2.9	1.1	6.08
	0.65	0.03	1.01	3.55	0.02	1.09	3.14	1.05	5.52
	0.75	0.03	0.99	4.5	0.02	1.11	2.64	1.05	5.37
	0.85	0.03	0.84	3.8	0.02	1.33	5.97	1.05	5.15
	0.9	0.02	0.81	3.5	0.02	1.19	5.06	1	5.08
	0.95	0.02	0.91	3.79	0.01	1.09	3.87	1	4.63
$I = \frac{3}{2} \ I_{\pi K}^f = \frac{3}{2} \ \pi K \rightarrow \pi\pi K$	0	0.13	0.81	5.5	0.11	1.52	6.67	1.1	6.36
	0.65	0.1	0.67	4.29	0.1	1.31	5.2	1	5.87
	0.75	0.1	0.69	4.51	0.1	1.24	4.3	1	5.35
	0.85	0.12	0.68	5.27	0.1	1.28	5.72	0.85	5.15
	0.9	0.11	0.68	5.36	0.1	1.19	5.56	0.8	4.89
	0.95	0.12	0.78	5.66	0.06	1.26	5	0.8	4.38
$I = \frac{3}{2} \ I_{\pi K}^f = \frac{1}{2} \ \pi K \rightarrow \pi\pi K$	0	0.35	0.84	5.17	0.34	1.66	4.84	1.2	5.8
	0.65	0.29	0.73	3.94	0.27	1.5	4.18	1.1	6.62
	0.75	0.3	0.7	4.62	0.3	1.44	4.27	1.05	5.97
	0.85	0.3	0.69	5.04	0.3	1.36	4.49	0.95	5.82
	0.9	0.29	0.67	5.51	0.29	1.3	4.81	0.85	5.49
	0.95	0.27	0.77	6.41	0.21	1.23	3.59	0.85	5.24

Table 4: The same as Table 3, but for four other reactions

Reactions	T/T_c	a_1	b_1	e_1	a_2	b_2	e_2	d_0	$\sqrt{s_z}$
$I = \frac{3}{2} I_{KK}^f = 1 \pi K \rightarrow K K \bar{K}$	0	0.02	0.6	3.92	0.02	1.08	2.82	0.75	6
	0.65	0.02	0.68	3.75	0.02	0.95	2.15	0.75	5.85
	0.75	0.03	0.69	3.01	0.01	1.19	2.69	0.75	5.64
	0.85	0.02	0.52	3.65	0.02	1.03	4.07	0.75	5.6
	0.9	0.01	0.43	3.19	0.02	0.87	3.57	0.65	5.49
	0.95	0.01	0.6	3.22	0.01	0.75	1.87	0.6	4.26
$I = 1 I_{\pi K}^f = \frac{3}{2} K K \rightarrow \pi K K$	0	0.46	0.65	3.43	0.38	1.26	3.11	0.95	6.15
	0.65	0.38	0.64	2.63	0.27	1.16	2.52	0.8	5.91
	0.75	0.4	0.55	3.08	0.35	1.14	3.47	0.8	5.54
	0.85	0.41	0.47	4.2	0.41	1.03	3.81	0.6	5.52
	0.9	0.4	0.45	4.69	0.39	0.94	3.93	0.6	5.49
	0.95	0.38	0.51	4.4	0.25	0.9	3.67	0.5	4.3
$I = 1 I_{\pi K}^f = \frac{1}{2} K K \rightarrow \pi K K$	0	0.07	0.92	3.64	0.03	1.44	3.16	1.05	6.49
	0.65	0.07	0.83	3.13	0.02	1.56	4.55	0.95	6.72
	0.75	0.05	0.73	3.22	0.04	1.21	3.54	0.9	6.27
	0.85	0.05	0.67	3.63	0.04	1.15	3.72	0.85	5.52
	0.9	0.04	0.54	4.52	0.05	1.04	4.58	0.75	5.08
	0.95	0.04	0.58	4.41	0.03	1.08	5.14	0.7	4.53
$I = 1 I_{\pi \bar{K}}^f = \frac{3}{2} K \bar{K} \rightarrow \pi K \bar{K}$	0	0.52	0.83	3.01	0.38	1.61	3.38	1.05	6.3
	0.65	0.44	0.84	2.52	0.23	1.51	2.54	1	6.18
	0.75	0.42	0.73	2.72	0.3	1.45	3.27	1	6.05
	0.85	0.37	0.57	3.56	0.38	1.26	3.7	0.85	5.66
	0.9	0.34	0.53	3.81	0.32	1.16	3.7	0.65	5.64
	0.95	0.28	0.56	4.01	0.22	1.09	3.68	0.6	5.22